

ISSN 2414-2352

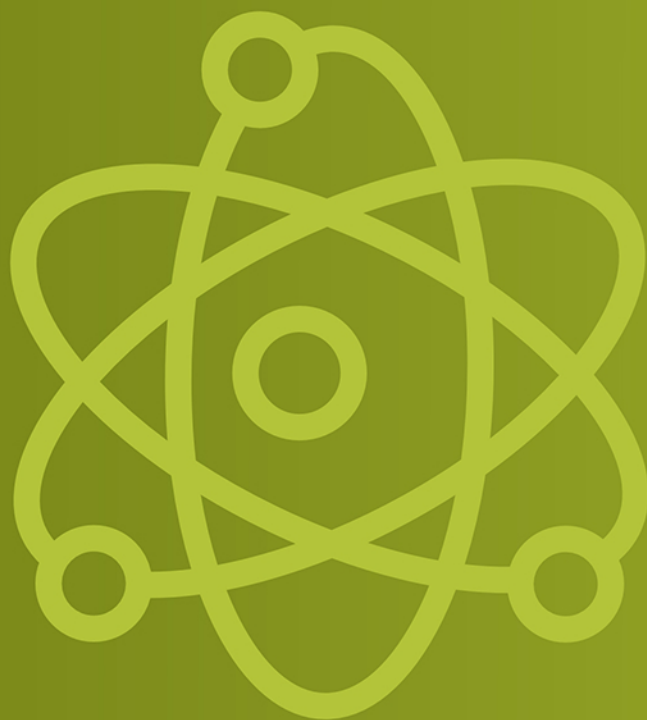


# The European Journal of Technical and Natural Sciences

Premier Publishing s.r.o.

2024

1 2 3 4 5 6



# **European Journal of Technical and Natural Sciences**

**2024, No 1**

# European Journal of Technical and Natural Sciences

Scientific journal

№ 1 2024

ISSN 2414-2352

## Editor-in-chief

**Hong Han**, China, Doctor of Engineering Sciences

## International editorial board

**Agaev Akbar**, Azerbaijan, Doctor of Chemical Sciences, Professor,  
Sumgayit State University

**Atayev Zagir**, Russia, Ph.D. of Geographical Sciences,  
Dagestan State Pedagogical University

**Boselin S.R. Prabhu**, India, Associate Professor, Surya Engineering  
College

**Buronova Gulnora**, Uzbekistan, PhD in Pedagogical science  
(computer science), Bukhara State University

**Chiladze George Bidzinovich**, Georgia, Doctor of Juridical Sciences,  
Doctor of Engineering Sciences, Akhaltsikhe State University, Tbilisi  
University

**Gevorg Simonyan, Armenia**, Candidate of chemical science, Associate  
professor, Yjevan Branch of Yerevan State University

**Giorgi (Gia) Kvinikadze**, Georgia, Doctor of Geographical Sciences,  
Tbilisi State University named after Ivane Javakishvili

**Kurdzeka Aliaksandr**, Kazakhstan, Doctor of Veterinary Medicine,  
Kazakh National Agrarian University

**Kushaliyev Kaissar Zhalitovich**, Kazakhstan, Doctor of Veterinary  
Medicine, Zhangir Khan Agrarian Technical University

**Manasaryan Grigoriy Genrihovich**, Armenia, Doctor of Technical  
Sciences, Armenian National Polytechnic University

**Nagiyev Polad Yusif**, Azerbaijan, Candidate of Agricultural Sciences,  
Sciences Institute for Space Research of Natural Resources, National  
Aerospace Agency

**Nikitina Veronika Vladlenovna**, Russia, Doctor of Medical Sciences,  
Associate Professor, PSPb State Medical University named after Academician  
I.P. Pavlov of the Ministry of Health of the Russian Federation

**Ogirko Igor Vasilievich**, Ukraine, Doctor of Physical and Mathematical  
Sciences, Ukrainian Academy of Press

**Petrova Natalia Guryevna**, Russia, Professor, Doctor of Medical  
Sciences, First St. Petersburg State Medical University named after I.P. Pavlov

**Rayiha Amenzade, Azerbaijan**, Dr. Sc. (Architecture), professor,  
Institute of Architecture and Art of ANAS (Azerbaijan)

**Sharipov Muzafar**, Uzbekistan, PhD in technical science, Associate  
professor, Bukhara State university

**Suleyman Suleymanov**, Uzbekistan, Senior Researcher, Associate  
Professor, PhD in Medical science, Bukhara State Medical University

**Tashpulatov Salih Shukurovich**, Uzbekistan, Doctor of Engineering  
Sciences, Tashkent Institute of Textile and Light Industry

**Vijaykumar Muley**, India, Doctor of Biological Sciences, Institute of  
Neurobiology, National Autonomous University of México (UNAM)

**Yarashev Kuvondik Safarovich**, Uzbekistan, Doctor of Geographical  
Sciences (DSc), Director, Urgut branch of Samarkand State University  
named after. Sharaf Rashidov

**Zagir V. Atayev**, Russia, PhD of Geographical Sciences, Dagestan State  
Pedagogical University

## Proofreading

Kristin Theissen

## Cover design

Andreas Vogel

## Additional design

Stephan Friedman

## Editorial office

Premier Publishing s.r.o.

Praha 8 – Karlín, Lyčkovo nám. 508/7, PSČ 18600

## E-mail:

pub@ppublishing.org

## Homepage:

ppublishing.org

**European Journal of Technical and Natural Sciences** is an international, English language, peer-reviewed journal. The journal is published in electronic form.

The decisive criterion for accepting a manuscript for publication is scientific quality. All research articles published in this journal have undergone a rigorous peer review. Based on initial screening by the editors, each paper is anonymized and reviewed by at least two anonymous referees. Recommending the articles for publishing, the reviewers confirm that in their opinion the submitted article contains important or new scientific results.

Premier Publishing s.r.o. is not responsible for the stylistic content of the article. The responsibility for the stylistic content lies on an author of an article.

## Instructions for authors

Full instructions for manuscript preparation and submission can be found through the Premier Publishing s.r.o. home page at: <http://ppublishing.org>.

## Material disclaimer

The opinions expressed in the conference proceedings do not necessarily reflect those of the Premier Publishing s.r.o., the editor, the editorial board, or the organization to which the authors are affiliated.

Premier Publishing s.r.o. is not responsible for the stylistic content of the article. The responsibility for the stylistic content lies on an author of an article.

## Included to the open access repositories:



Crossref

eLIBRARY.RU

Google Scholar

H – 15 and more than 500  
citations in international  
periodicals and monographs.



The journal has Index Copernicus Value (ICV) 92.08 for 2022.

## © Premier Publishing

All rights reserved; no part of this publication may be reproduced, stored in a retrieval system, or transmitted in any form or by any means, electronic, mechanical, photocopying, recording, or otherwise, without prior written permission of the Publisher.



## Section 1. Electrical engineering

DOI:10.29013/EJTNS-24-1-3-10



### THERMAL AND ENERGY CHARACTERISTICS OF A COGENERATIVE FRACTAL SOLAR COLLECTOR

**Rustamov Nasim Tulegenovich<sup>1</sup>,  
Kibishov Adylkhan Talgatovich<sup>1</sup>, Mukhamejanov Nuridin Bakhtiyaruly<sup>1</sup>**

<sup>1</sup> International Kazakh-Turkish University named after Khoja Ahmed Yasawi,

---

**Cite:** Rustamov, N.T., Kibishov, A.T., Mukhamejanov, N.B. (2024). Thermal and Energy Characteristics of a Cogenerative Fractal Solar Collector. *European Journal of Technical and Natural Sciences* 2024, No 1. <https://doi.org/10.29013/EJTNS-24-1-3-10>

---

#### Abstract

The paper considers the design and thermal energy characteristics of a new type of fractal solar collector operating in cogeneration mode. The principle of operation of the proposed solar installation is given. The efficiency of using solar insolation in comparison with flat solar collectors is shown.

**Keywords:** Fractal, solar collector, cogeneration mode, solar insolation, electric energy

#### Introduction

A solar collector is a device for collecting thermal energy from the Sun (solar installation), carried by visible light and near infrared radiation. Unlike solar panels, which produce electricity directly, the solar collector heats the coolant material.

As is known, thermal energy analysis is especially important for solar installations, since this natural source is characterized by stochasticity and strong energy dissipation in space, which requires a design change to increase the use of solar energy. The problem of the need to conduct an energy analysis of such installations was formulated in the works of P.L. Kapitsa.

The more incident energy is transferred to the coolant flowing in the collector, the higher

its efficiency. It can be increased by using special optical coatings that do not emit heat in the infrared spectrum. All existing solar collectors in the world differ mainly in their design, material and manufacturing technology of their absorbers (Avezova, N.R. Avezov, R.R., Rustamov, N.T., Vakhidov, A., Suleymanov, Sh.I., 2013; Ermuratsky, V.V., Postolatiy, V.M., Koptiyuk, E.P., 2009). At the same time, the option of increasing the efficiency of the collector by changing the location of the absorbers on the aperture area of the collector is not considered.

The development of efficient designs of solar collectors and installations for heat supply to the population, as well as the search for ways and new technologies that are economically advantageous for the use of solar heat supply

systems today, is one of the urgent problems of large-scale use of solar energy in the field of municipal thermal power engineering.

The purpose of the work is to increase the efficiency of using solar rays by solar collectors, due to their operation in a cogenerative mode.

### The solution method

The Department of Electrical Engineering of the A. Yassavi International Kazakh Turkish University has developed and patented several fundamentally new designs for the location of absorbers on the aperture area and their shape of solar collectors. In order to reduce heat loss and increase the energy efficiency of solar collectors, an optimal design has been developed, where absorbers in the form of fractals are located on the aperture area of a parabolic concentrator according to the principle of the Fibonacci number. Such a solar installation was called fractal solar collectors  $\Phi CK$  (Rustamov, N. T.,

Meirbekov, A. T., Korganbaev, B. N., Patent No. 2639; Rustamov, N. T., Meirbekov, A. T., Kibishev, A. T., invention No. 36213).

The aperture area of such a collector serves as a reflector of the sunlight passing through and past the absorbers. The reflected rays additionally heat the collector pipes arranged in the form of fractals. Thus, the sun's rays are used multiple times. As a result, the efficiency of the  $\Phi CK$  increases compared to a flat solar collector (Rustamov, N. T., Kibirov, A. T., Israilov, F. M., Ernazar, K. E., 2023; Rustamov, Nassim, Kibishov, Adylkhan, Naci Genc, Shokhrukh Babakhan, Ernazar Kamal, 2023).

This type of solar installation is a battery of a parabolic concentrator (similar in shape to a satellite dish), which focuses reflected sunlight from the aperture area onto receivers located at the focal point (the first fractal). In the presented case, the solar installation allows the consumer to receive m of thermal water of various temperatures.

**Figure 1.** Toroidal absorber: a), the general design of fractal solar collectors b) If the  $\Phi CK$  operates in cogeneration mode, the efficiency of the solar installation will increase even more.

Based on this concept, the department has developed a cogenerative fractal solar collector

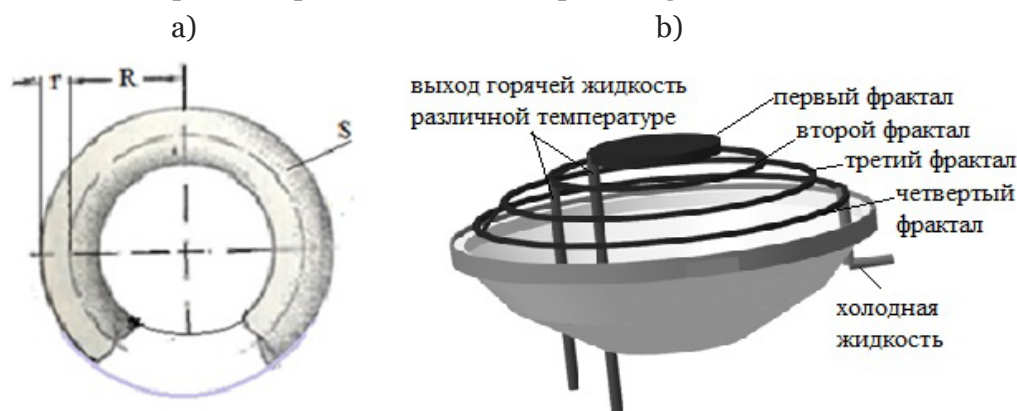
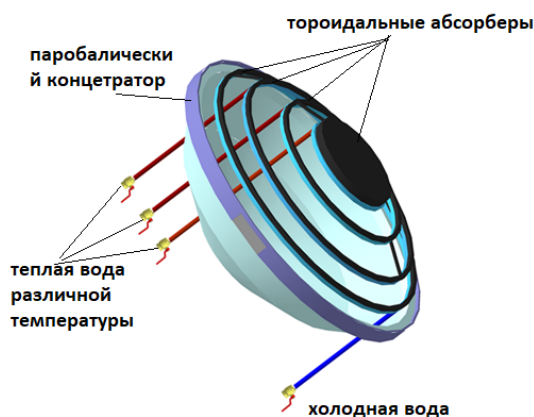


**Figure 2.** General view of a cogenerative fractal solar collector

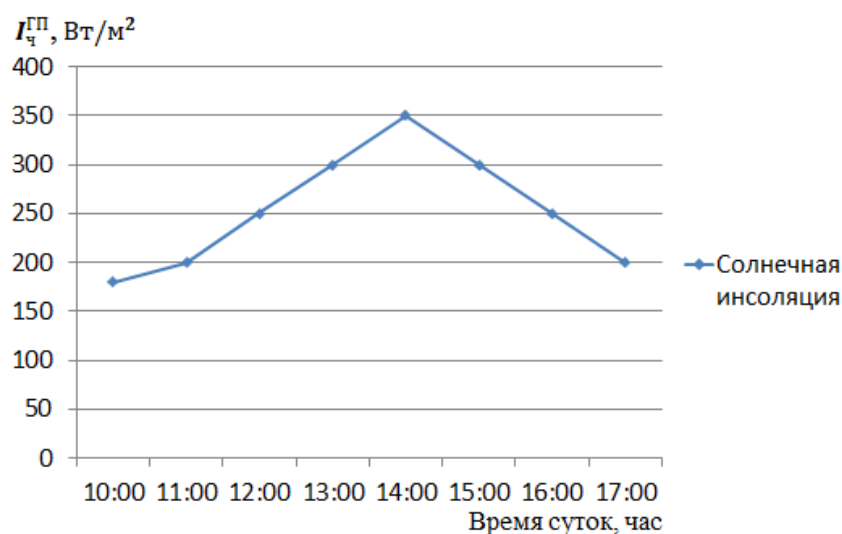


As is known, when a solar installation generates both electrical and thermal energy, then it is said that the solar installation operates in the mode of cognition. In order for the  $\Phi CK$  to work in cogeneration mode, the reverse side of the toroid absorber is sheathed with a polymer photo panel. Then the reflected rays from the aperture area of the collector colliding with the photo panel will generate an electric current. As a result, the  $\Phi CK$  starts working in cogeneration mode.

During the operation of the  $K\Phi CK$ , the consumer will receive heat and electricity at the same time, this is the cogeneration of the

solar installation. To assess the thermal and energy characteristics, the  $K\Phi CK$  was manufactured according to the method described in (Rustamov, Nassim, Kibishov, Adylkhan, Naci Genc, Shokhrukh Babakhan, Ernazar Kamal, 2023). Based on the experimental data obtained, the ability of the  $K\Phi CK$  to absorb solar radiation, the useful power of solar radiation for a solar collector, heat losses, and the electrical power that the solar installation generates were evaluated. All calculations were carried out for solar insolation for the city of Turkestan for the month of March 2023. (Fig. 3).

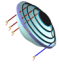
**Figure 3.** Daily solar insolation for Turkestan (1.03.2023)

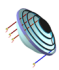


The electrical characteristics of the  $K\Phi CK$  were measured every hour. The electric current generated by the solar panels was

measured for each fractal of the  $K\Phi CK$ . The estimates obtained are shown in Table 1.

**Table 1.** Energy characteristics in  $K\Phi CK$

<b><math>K\Phi CK</math> Energy description</b> 	<b>Daily hours</b>							
	<b>10<sup>00</sup></b>	<b>11<sup>00</sup></b>	<b>12<sup>00</sup></b>	<b>13<sup>00</sup></b>	<b>14<sup>00</sup></b>	<b>15<sup>00</sup></b>	<b>16<sup>00</sup></b>	<b>17<sup>00</sup></b>
$I_{\text{с}}^{\text{П}}, W / m^2$	180	200	250	300	350	300	250	200
$R$	2.56	2.18	2.09	2	2	2.09	2.18	2.56
$t_{\text{окр}}, ^\circ C$	8	9	10	11	12	13	14	13
$I_{\text{с}}^{\text{ПП}}, W / m^2$	460.8	436	522.5	600	700	627	549.4	512
$I_{\text{с}}^{\text{нозл}}, W / m^2$	354.8	335.7	402.3	462	539	482.8	423	394.2
$\gamma_{\text{с}}^{\text{mn}}, W / m^2$	312	306	300	294	288	282	276	282
$Q_{\text{л}1}^{\text{у}}, W / m^2$	5	8.5	21.9	39.6	60.4	49.5	34.2	24.1

КФСК Energy description 	Daily hours							
	10 <sup>00</sup>	11 <sup>00</sup>	12 <sup>00</sup>	13 <sup>00</sup>	14 <sup>00</sup>	15 <sup>00</sup>	16 <sup>00</sup>	17 <sup>00</sup>
$Q_{l_{a2}}^u, W / m^2$	6.2	10.3	24.7	46.2	78.1	56.9	34.2	26.2
$Q_{l_{a3}}^u, W / m^2$	7.3	12	37.5	50.7	86	66.3	36.1	34.2
$Q_{l_{отр}}^u, W / m^2$	14.7	15.9	17.2	18.4	19.6	21	19.6	17.2
$Q_{обмт}^u, W / m^2$	16.8	18.2	19.6	21	22.4	23.8	22.4	19.6
$\eta_u^{a_1}, \%$	21	22.8	24.5	26.3	35	29.8	28	24.5
$\eta_u^{a_2}, \%$	52.5	56.9	61.3	65.7	77	74.6	70	61.3
$\eta_u^{a_3}, \%$	71	84	145.4	202.2	301.5	247.3	174.5	145.8
$\eta_u^{omp}, \%$	60	70	74	75.4	76	75.3	75	74.6

First of all, we measure the radius of each fractal located in the solar collector,  $R_1, R_2, R_3$ , and the inner radius of the fractal tube  $r$ .

$R_1 = 0.15$  m,  $R_2 = 0.30$  m,  $R_3 = 0.40$  m,  $r = 0.016$  m.

Using the measured radii, we calculate the surface area of each fractal pipeline

$A_{a_1}, A_{a_2}, A_{a_3}$ .  
 $A_{a_1} = 0.13$  m<sup>2</sup>;  $A_{a_2} = 0.19$  m<sup>2</sup>;  $A_{a_3} = 0.25$  m<sup>2</sup>;

The hourly values of the useful part of the solar radiation power are found by the formula,  $F_R = 0.9$

$$Q_{l_{a1}}^u = A F_R (I_u^{nozл} - \gamma_u^{mn})$$

Where

$A$  – absorber

$F_R$  – is the heat transfer coefficient from the solar collector

$I_u^{nozл}$  – the corresponding hourly values of absorbed solar radiation

$\gamma_u^{mn}$  – hourly value of heat losses

For the first absorber

$$\begin{aligned} Q_{l_{a1}}^{12^{00}} &= A_{a_1} F_R (I_{12^{00}}^{nozл} - \gamma_{12^{00}}^{mn}) = \\ &= 0.13 * 0.9 (704,8 - 300) = 47.4 \text{ W} / \text{m}^2 \end{aligned}$$

For the second absorber

$$\begin{aligned} Q_{l_{a2}}^{12^{00}} &= A_{a_2} F_R (I_{12^{00}}^{nozл} - \gamma_{12^{00}}^{mn}) = \\ &= 0.19 * 0.9 (704,8 - 300) = 69.2 \text{ W} / \text{m}^2 \end{aligned}$$

For the second absorber

$$\begin{aligned} Q_{l_{a3}}^{12^{00}} &= A_{a_3} F_R (I_{12^{00}}^{nozл} - \gamma_{12^{00}}^{mn}) = \\ &= 0.25 * 0.9 (704,8 - 300) = 91.1 \text{ W} / \text{m}^2 \end{aligned}$$

We determine the area of the solar panel under each absorber  $A_1, A_2, A_3$

We determine the area of the solar panel under the first absorber  $A_1$

$R_1$  – is the first radius of the fractal (0.15 m)

$$A_1 = \pi R_1^2 = 3.14 * 0.15^2 = 0.07 \text{ m}^2$$

The area of the solar panel under the second absorber is determined by the formula  $A_2$

$$A_2 = l_2 * a$$

First of all, we measure the length of the second fractal  $l_2 = 2\pi R_2$   $R_2 = 0,3$  m

$$l_2 = 2\pi R_2 = 2 * 3.14 * 0,3 = 1.9 \text{ m}$$

Now let's determine the area of the solar panel under the second absorber  $A_2$

$$A_2 = l_2 * a$$

$a$  – the width of the solar panel,  $a = 0.04$  m

$$A_2 = l_2 * a = 1.9 * 0.04 = 0.08 \text{ m}^2$$

We determine the area of the solar panel under the third absorber  $A_3$

We measure the length of the third fractal  $l_3 = 2\pi R_3$  where  $R_3 = 0,4$  m

$$l_3 = 2\pi R_3 = 2 * 3.14 * 0,4 = 2.6 \text{ m}$$

The area of the solar panel under the third absorber is determined by the formula

$$A_3 = l_3 * a$$

$$A_3 = l_3 * a = 2.6 * 0.04 = 0.1 \text{ m}^2$$

The power of the solar panel is determined by the formula P

$$P = A * \eta * I_{\text{лyч}} \quad (9)$$

where

$A$  – solar panel area m<sup>2</sup>

$\eta$  – the percentage of solar panel efficiency of 15% is 0.15



$I_{\text{луч}}$  – radiance is the radiant power of reflected solar radiation  $W / m^2$

We find the area of the area of reflection of sunlight

$$\begin{aligned} A_{\text{пар}} &= \pi(h^2 + 2a^2) = \\ &= 3.14 * (0.25^2 + 2 * (0.40)^2) = 1.2 m^2 \\ A_{\text{абсор}} &= A_1 + A_2 + A_3 = 0.13 + 0.19 + \\ &+ 0.25 = 0.57 m^2 \end{aligned}$$

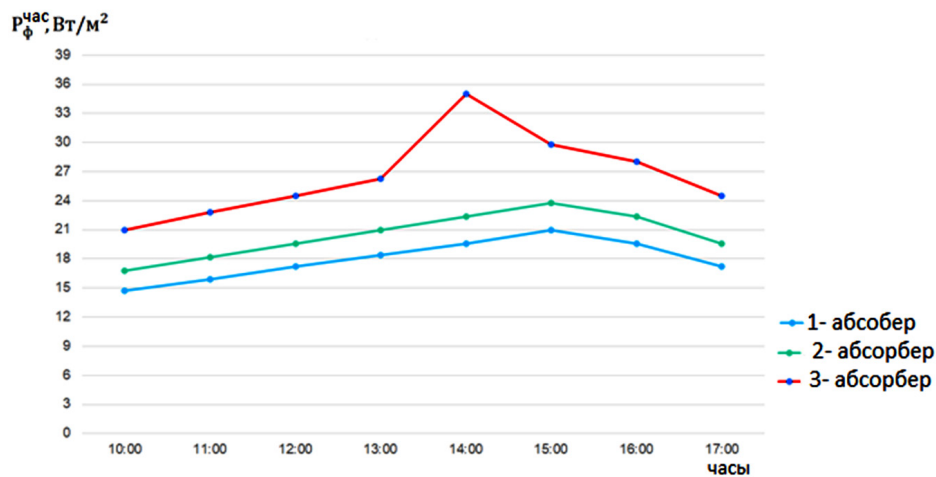
$$A_{\text{кв.плоск}} = A_{\text{пар}} - A_{\text{абсор}} = 1.2 - 0.57 = 0.63 m^2$$

Calculate the value of reflected solar radiation from a parabolic concentrator,  $F_R = 0.9$ ;

$$A_{\text{кв.плоск}} = 0.63 m^2.$$

$$\begin{aligned} I_{\text{луч}}^{12^{00}} &= A_{\text{у.у.}} F_R (I_{12^{00}}^{\text{ж.у.м}} - \gamma_{12^{00}}^{\text{ТП}}) = \\ &= 0.63 * 0.9 (704.8 - 300) = 229.5 W / m^2 \end{aligned}$$

**Figure 4.** Graph of the electric power on the solar panel in each fractal of the КФСК by the hour



Doubles the value of solar radiation reflected from a parabolic concentrator

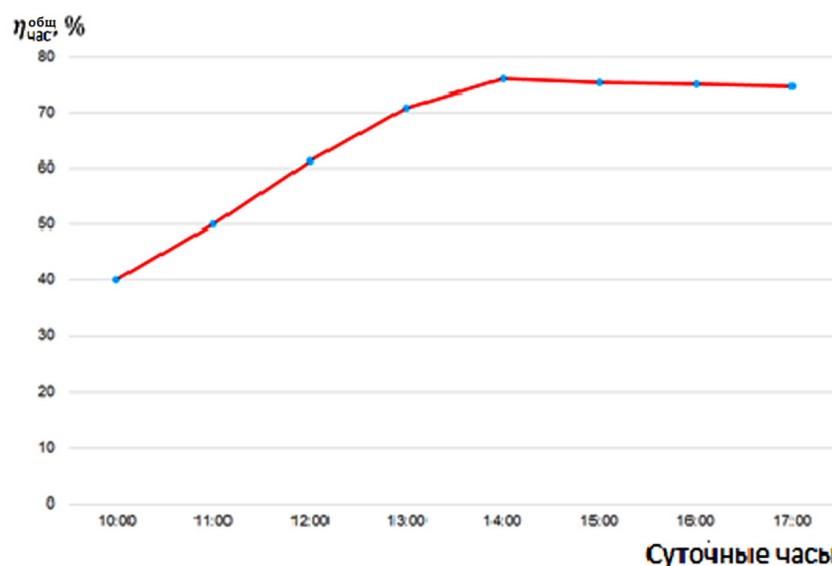
Using formula (9), we find the power of the solar panel on each fractal of the КФСК  $P_1, P_2, P_3$

$$\begin{aligned} P_1 &= A_1 * \eta * I_{\text{луч}}^{12^{00}} = \\ &= 0.07 * 0.35 * 700 = 17.2 W \end{aligned}$$

$$\begin{aligned} P_2 &= A_2 * \eta * I_{\text{луч}}^{12^{00}} = \\ &= 0.08 * 0.35 * 700 = 19.6 W \end{aligned}$$

$$\begin{aligned} P_3 &= A_3 * \eta * I_{\text{луч}}^{12^{00}} = \\ &= 0.1 * 0.35 * 700 = 24.5 W \end{aligned}$$

**Figure 5.** Dynamics of efficiency by daily hours to КФСК





We calculate the total power received from the solar panel from КФСР at 12:00  $P_{общ}$

$$P_{общ} = P_1 + P_2 + P_3 = 17.2 + 19.6 + 24.5 = 61.3 \text{ W}$$

Analyzing this graph, we can add that the generation of electric energy using a water-heating solar installation has a number of advantages. Our experiments have shown that the generated electric energy by a water-heating solar installation can meet the needs of the solar installation itself. Thus, we can verify the effectiveness of the КФСР. Below we present the dynamics of efficiency changes.

An assessment of such dynamics of a water heating solar installation makes it possible for the consumer to optimize the operating time of this solar installation.

As an example, we will show the dynamics of the efficiency of a cogenerative fractal solar collector in eight hours. To do this, we selected the following initial values from Table 1.

$$I_{12^{00}}^{HII} = 555.5 \frac{\text{Bm}}{\text{M}^2}; Q_{общ}^{12^{00}} = 196.5 \frac{\text{Bm}}{\text{M}^2};$$

$$P_{общ}^{12^{00}} = 17.25 \text{ W};$$

The efficiency for the CFSC as a whole, where we determined the total area of the solar panel  $A_{\text{кв.плот}} = 0.63 \text{ M}^2$

$$\eta_{12^{00}}^{общ} = \frac{Q_{общ}^{12^{00}} + P_{общ}^{12^{00}}}{A_{общ} I_{12^{00}}^{HII}} * 100 =$$

$$= \frac{196.5 + 61.3}{0.63 * 555.5} * 100 = 74\%$$

Taking into account the corresponding hourly electrical values of the КФСР  $Q_{общ}^u$  and  $I_u^{HII}$ , their daily (total) values are determined by the formulas  $Q \Sigma Q_{общ}^u$  и  $\Sigma I_u^{HII}$ , using formula (9), we found the daily efficiency of CFSC:

$$\eta_{\text{КФСР}_{\text{сут}}} = \frac{\Sigma Q_{общ}^u}{A_{\text{абсор}} \Sigma I_u^{HII}} * 100 =$$

$$= \frac{71 + 84 + 145.4 + 202.2 + 301.5 + 247.3 + 174.5 + 145.8}{0.63 * (460.8 + 436 + 522.5 + 600 + 700 + 627 + 549.4 + 512)} * 100 =$$

$$= \frac{1371.7}{4407.7 * 0.48} * 100 = 71.3\%$$

Using the following empirical formula in the КФСР, we determined the average daily value of efficiency:

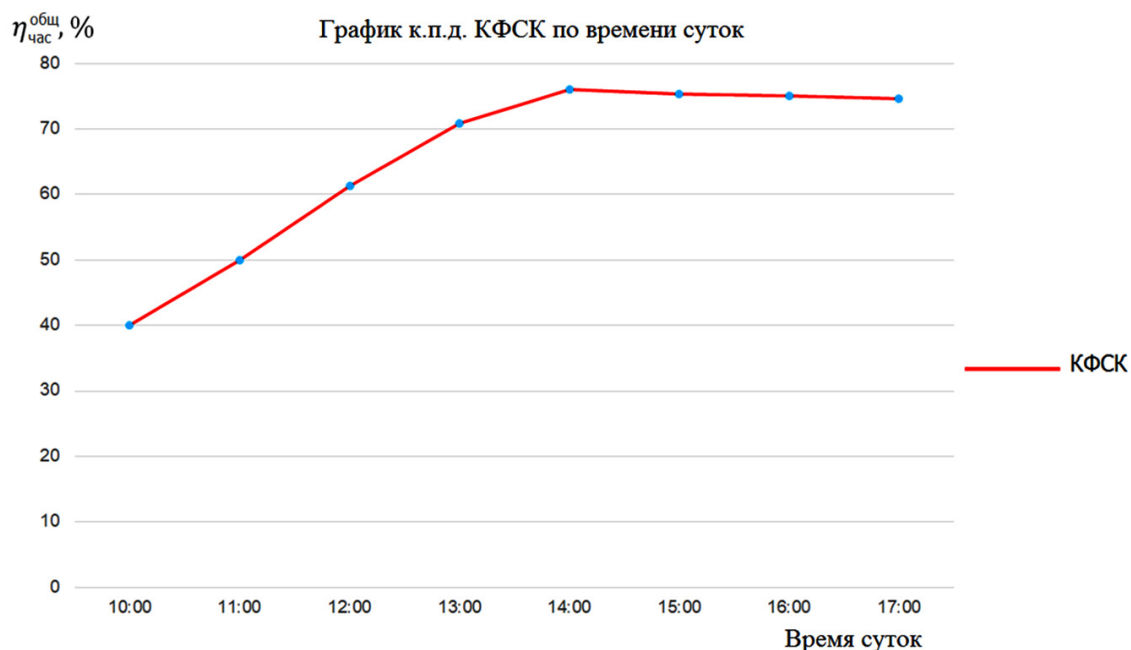
$$\eta_{\text{КФСР}_{\text{сут}}}^{\text{сред}} = \frac{\Sigma \eta_{общ}}{n} =$$

$$= \frac{71 + 84 + 145.4 + 202.2 + 301.5 + 247.3 + 174.5 + 145.8}{24} =$$

$$= 58.3\%$$

where  $\eta_{общ} = \Sigma \eta_{\text{час}}$  – the hourly efficiency values in the КФСР are taken from Formula (7).

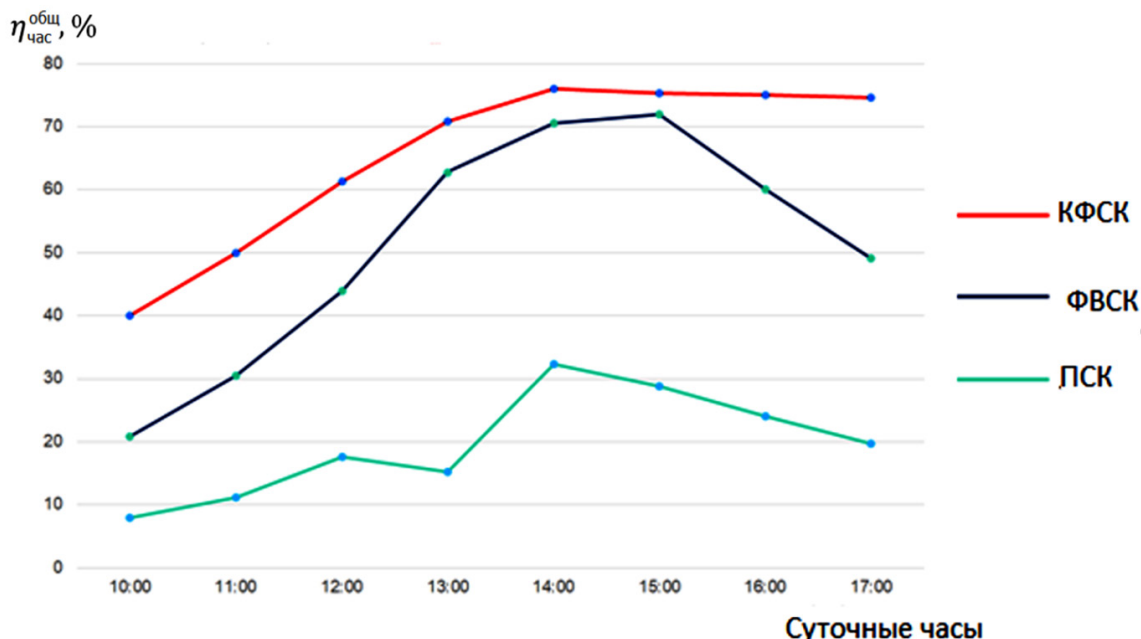
**Figure 6.** Dynamics of changes in the efficiency of a cogenerative fractal solar collector



Now let's consider a retrospective analysis of the efficiency of three solar collectors ПСК, БФСК and КФСК. The efficiency data for a fractal evacuated collector (ФБСК) and

a flat solar collector (ПСК) are taken from (Rustamov, Nassim, Kibishov, Adylkhan, Naci Genc, Shokhrukh Babakhan, Ernazar Kamal, 2023).

**Figure 7.** Retrospective analysis of the efficiency of three solar installations



This graph confirms the concept that was given at the beginning of the article. The positive and negative results obtained during the experiments stimulate the further development of research in this direction.

### Conclusions

The use of solar collectors due to solar energy can reduce the cost of heating and hot water. Recent studies have shown that by changing the design of the absorbers in the aperture area, the use of solar insolation in a solar installation can increase its efficiency. The efficiency of installations performed with

such a design can reach 80–85%. The new type of solar collector described in this paper is called a cogenerative fractal solar collector (КФСК). On the other hand, the creation of a КФСК producing both heat and electricity will stimulate the further development of solar collectors.

According to the results of the experiment, it can be said that the КФСК has shown itself to be on the good side in terms of the simplicity of its design and the low cost of consumable material, small footprint, and the efficiency of using solar insolation.

### References

- Avezova, N.R. Avezov, R.R., Rustamov, N.T., Vakhidov, A., Suleymanov, Sh.I. Resource indexes of flat solar water-heating collectors in hot-water supply systems: 4. Specific collector thermal yield and efficiency. Journal Applied Solar Energy, 2013.— Vol. 49.— Issue 4.— P. 202–210.
- Ermuratsky, V.V., Postolatiy, V.M., Koptiyuk, E.P. Prospects of application of solar water heaters for sanitary purposes in the Republic of Moldova. Problems of regional energy. 2009.— № 2. URL: [http://ieasm.webart.md/data/m71\\_2\\_107.doc](http://ieasm.webart.md/data/m71_2_107.doc)
- Rustamov, N.T., Meirbekov, A.T., Korganbaev, B.N. Fractal solar collector. RK, Patent. — No. 2639 for a utility model.
- Rustamov, N.T., Meirbekov, A.T., Kibishev, A.T. Vacuum fractal solar collector. Patent of the Republic of Kazakhstan for invention No. 36213.

- Rustamov, N. T., Kibirov, A. T., Israilov, F. M., Ernazar, K. E. Efficiency coefficient of a vacuum fractal solar collector. European Journal of Technical and Natural Sciences — 2. 2023.— P. 46–53.
- Rustamov, Nassim, Kibishov, Adylkhan, Naci Genc, Shokhrukh Babakhan, Ernazar Kamal. Thermal Conductivity of a Vacuum Fractal Solar Collector. International Journal of Renewable Energy Research N,— Vol. 13.— No. 2.— June, 2023.— P. 613–618.

submitted 22.08.2024;

accepted for publication 20.09.2024;

published 8.10.2024

© Rustamov, N. T., Kibishov, A. T., Mukhamejanov, N. B.

Contact: babakhan.shokhrukh@ayu.edu.kz



## Section 2. Medical science

DOI:10.29013/EJTNS-24-1-11-15



### ASSOCIATED SOMATIC DISEASES IN PATIENTS WITH CERVICAL CANCER (SAMPLE ARTICLE)

**Polatova D. Sh.<sup>1</sup>, Artikhodzhaeva G. Sh.<sup>2</sup>**

<sup>1</sup>Tashkent State Dental Institute, Center for Pediatric  
Hematology, Oncology and Clinical Immunology

<sup>2</sup>Tashkent State Dental Institute, Center for Professional  
Development of Medical Workers

---

**Cite:** Polatova D. Sh., Artikhodzhaeva G. Sh. (2024). Associated Somatic Diseases in Patients With Cervical Cancer (Sample Article). *European Journal of Technical and Natural Sciences* 2024, No 1. <https://doi.org/10.29013/EJTNS-24-1-11-15>

---

#### Abstract

Disturbance of the balance of sex hormones leads to atrophic or hypertrophic degeneration of genital tissues. To study the hormonal background in vaginal cancer, we studied the level and ratio of estrogen metabolites in vaginal cancer, as in other cancer localizations.

#### Keywords:

#### Introduction

**Enter** As mentioned above, the imbalance of sex hormones leads to atrophic or hypertrophic degeneration of the tissues of the

genital organs. To study the hormonal background in vaginal cancer, we studied the level and ratio of estrogen metabolites in vaginal cancer, as in other cancer localizations.

**Table 1.** Levels and ratios of estrogen metabolites: 16 $\alpha$ -ONE1 and 2-ONE1 in vaginal cancer

Mean level of metabolites (ng/ml)	Cancer patients	Control group
2-OHE1	14.02 $\pm$ 3.17	28.12 $\pm$ 8.30
16 $\alpha$ -OHE1	19.91 $\pm$ 5.74	9.33 $\pm$ 2.49
2-OH1/16 $\alpha$ -OH1	0.70 $\pm$ 0.55	3.01 $\pm$ 0.33

From the data presented in the table, it can be seen that with vaginal cancer, as in other tumor localizations, there is a clear imbalance in the hormonal picture compared

to the control group. In the case of Qin cancer, the mean level of metabolite 2-ONE in the patient group was 2.38 times lower than that of the control group. Meanwhile, the av-

erage level of metabolite 16 $\alpha$ -ONE was 2.13 times higher than that of the control group. The proportions of metabolites in the groups also showed significant, statistically significant ( $P < 0.01$ ) differences. In the control group, the value of 2-ONE / 16 $\alpha$ -ONE was 4

(4.49) times higher than the same coefficient for patients with vulvar cancer. The somatic condition of women with genital cancer did not differ from the somatic health of women with cancer elsewhere (Table 2).

**Table 2.** Comorbidities of women with vaginal cancer were included in the study

Nosological form	Number of patients
Obesity	9 (56.3%)
Hypertension disease	5 (31.3%)
IUD	2(12.5%)
US diseases*	8 (50%)
Hypothyroidism	1 (6.3%)
GT diseases *	6 (37.5%)
Chronic hepatitis	2 (12.5%)
Hepatositis	4 (25%)
COLD *	6 (37.5%)
<b>Total</b>	<b>43 (268.8%)</b>

\* Note: IUD is an ischemic heart disease; US – urinary system; GT – gastrointestinal tract; COLD – chronic obstructive lung disease

Often, patients with vaginal cancer suffer from obesity, inflammatory diseases of the urinary system (chronic pyelonephritis, cystitis) and chronic obstructive pulmonary diseases. It is known that in addition to the respiratory function, the lungs also perform endocrine functions. Lung tissue releases biologically active substances such as fibrinolytin. Also, lung tissue plays an important role in processes such as hormone production, water-salt and lipid metabolism. Blood collects in the vascular system of the lungs. The respiratory system also provides immunity against harmful environmental factors. In this regard, during the general improvement of the patient's body, the accompanying lung disease should not be neglected.

Microscopic examination of vaginal discharge to detect vaginal infections (for example, trichomoniasis, bacterial vaginosis, candidiasis), on the basis of which the cleanliness of the smear is evaluated in the studied patients. Most cervical cancer patients have an abnormal smear during the initial examination. Thus, the cleanliness of the smear of the third degree was detected in 64.5% of patients, in 21.1% of patients of the fourth degree, a pathological smear was detected in 85.6% of patients. Treatment did

not improve smear purity; more pronounced deviations regarding contamination during radiation therapy were noted; pathological smear was observed in 65.7% of patients before radiation therapy; during the treatment and after the end of radiation, 86.9% of patients had a worsening of the microbiocenosis, with chemotherapy, this figure was 63.3% before treatment and 71.4% after it. Despite the use of antibiotics during surgical treatment, smear purity deteriorated from 59.4% to 65.6%, mainly due to the growth of yeast-like fungal colonies and necrotic masses. The content of many bacteria was pathologically high. For example, gardnerella is a saprophytic (conditional pathogen) infection, but with an increase in their number, it causes inflammation, reduces protective functions, local immunity, which creates a favorable environment for the attachment and reproduction of other pathogenic microorganisms and promotes their emergence. the development of diseases such as colpitis, cervical ectopia, less often – leukoplakia, cervicitis, adnexitis, endometriosis, cystitis and pyelonephritis. In every second case, genital chlamydia was detected in smears, which contributes to the development of diseases such as endometritis, salpingo-oophoritis, and salpingitis.

### The main part

In our study, overgrowth of *Candida albicans* was detected in 30.1% of cases. All patients (104 patients) who did not receive additional therapy for various reasons during the main course of treatment aimed at combating an established infection were microbiologically examined, mainly those who received chemotherapy (49 patients) and radiation (8 patients). Treatment with specialized UV light led to the worsening of the microbiocenosis in the cervix and vagina. Severe microbiological damage to the organ was noted. The number of *Candida albicans* and *Gardnerella* increased by two, *Ureaplasma* (*Ureaplasma urealyticum* i *Ureaplasma parvum*.) increased by more than 22%, and high titers of genital chlamydia increased dramatically. *Ureaplasma* produces a special enzyme that causes the breakdown of immunoglobulin A, thereby reducing immunity against infection. We looked for different types of human papillomavirus in all 161 patients with cervical cancer. In cervical cancer, mainly human papillomavirus types 16 and 18 (HPV-16, HPV-18) are identified. These are high-risk viruses; the second low-risk group is less often associated with malignant tumors (viruses 6, 11, 42, etc.). As shown in the table, cervical cancer patients were mainly affected by viruses of types 16 and 18, while dangerous (high) titer was detected in 64.6% of human papillomavirus type 16 and in almost 50% of titer of type 18. HPV was detected in 119 (73.9%) patients, and 16 types of the virus were detected in all cases. Of 119 (100%) patients, HPV-16 and 79 (66.4%) HPV-18 were detected at high titers in 104 (87.4%) patients. In 15 patients with a low titer of HPV-16 (12.6%), high titers of HPV-18 and 42 were noted. The special treatment carried out, for example, radiation and cytostatic therapy, contributed to the further deterioration of the microbiocenosis of the cervical canal and vagina. The hormonal level of 83 patients was checked (studied). Patients' blood and cervical biopsy materials were analyzed. Estrogen (estradiol), thyroid hormones, glycated hemoglobin, prolactin and progesterone levels were studied. In patients with uterine cancer, as well as cervical cancer, mainly 16 and 18 types of viruses were at a high level, dangerous (high)

titer of HPV-16 was detected in one third, 28.9% of 18 types. HPV was detected in 23 (51.1%) patients, 15 of them (33.3%) had high titers. Almost always, 2 or more types of viruses are found in patients with viral infection. The presence of hormonal receptors was also studied in patients with uterine cancer using an immunohistochemical method. Taking into account the high prognostic role, the receptors were identified, the presence of estrogen and progesterone receptors and HER-2 neu was determined. Our goal was not to study the prognostic role of IHC data, so we did not study the proliferative activity of the tumor and other factors. In 24.5% of patients, the average or high level of estrogen receptors, progesterone in 60% of patients, HER-2 neu was detected in 13.4% of patients, which was the basis for the use of antiestrogens, progestins and trastuzumab.

The most common condition in patients with endometrial cancer is obesity, which affects more than 75% of patients; the remaining patients are patients with a tendency to obesity, which is a link in the chain of metabolic syndrome observed in patients with uterine corpus. Although diabetes was observed in only 11.1% of patients, 23 (51.1%) patients had elevated blood glucose, which was evaluated as prediabetes and prescribed a special diet low in easily digestible carbohydrates. Also, many patients with uterine cancer are diagnosed with OSOK, chronic hepatitis and hepatosis. All patients with ovarian cancer underwent radical surgery. According to intraoperative data, 7 (11.1%) patients received postoperative radiation and all patients received 6 courses of polychemotherapy. The composition of microorganisms in the distal part of the upper genitals and fallopian tubes was studied (intraoperatively). The prevalence of *Gemmata obscuriglobus*, *Halobacteroides halobios* chlamydia, HPV, etc. was higher in ovarian cancer patients than in endometrial cancer patients. The following types of bacteria increase in ovarian cancer: *Proteobacterii*, *Acinetobacter*, *Sphingomonas*, *Methylobacterium* spp., *Vodnye vidy*, *planktomycety*, *Gemmata obscuriglobus*, *Halobacteroides halobius* i *Methyloprofundus sedimenti*, etc. High titers of these microorganisms can be an indirect sign of the presence and/or activity (aggressiveness) of ovarian cancer. We found



high titers of HPV in many patients with ovarian cancer. Diseases of the reproductive system and the hormonal level of women are closely related. Hormonal imbalance leads to functional failure of the receptor apparatus of the vulva. What can cause the development of anaplastic processes. Like other localizations of oncogynecological pathology, we studied hormonal disorders in patients with vulvar cancer, for which we determined the level and ratio of estrogen metabolites: 16 $\alpha$ -ONE1 and 2-ONE1, according to FIGO recommendations. For comparison, this test was conducted on 15 women from hospital staff. The mean level of 2-ONE metabolite in the group of patients with vulvar cancer was 2.38 times lower than that of the control group. At the same time, the average level of metabolite 16 $\alpha$ -ONE was 1.9 times higher than that of the control group. vulva. The proportions of metabolites in the groups also showed significant, statistically significant ( $P < 0.01$ ) differences. In the control group, the value of 2-ONE / 16 $\alpha$ -ONE was 4 (4.49) times higher than the same coefficient for patients with vulvar cancer. Thus, it is desirable to take measures on pathogenetic therapy of vulvar cancer, which will allow significant progress in the treatment of women with vulvar cancer. With cancer of the vulva, as in other localizations of gynecological oncological pathology, many chronic diseases and conditions were observed. According to our observations, obesity was observed in almost half of patients, gastrointestinal diseases and hepatosis were observed in one third of patients, hypertension was diagnosed in every fourth patient. Three patients experienced infertility.

We conducted a prospective study of 16 patients to base an adjunctive therapy program on rectal cancer. Of the 16 patients, 9

had primary Qin cancer, 7 developed after radiation therapy for cervical cancer (5 patients), and 2 patients developed vulvar cancer after treatment. At the current stage of medical development, the vaginal biocenosis is the most important component of the body that performs protective and immunomodulating functions. To study the microbiocenosis, we conducted a microbiological study of vaginal discharge and smears. With vaginal cancer, as with vulvar cancer, there is colonization of the vagina with pathological colonies that are more characteristic of intestinal flora. Also, a large number of cases were identified as genital chlamydia and gardnerellosis. In 75% of cases, bacterial infection was accompanied by yeast fungi.

### Summary

Based on our research, it can be noted that HPV plays a major role in the occurrence and development of genital cancer in women. For the prevention of malignant tumors of the vulva, vagina and cervix, a vaccination method is proposed today, but the effect on the pathogenetic mechanism of cancer in the treatment of advanced oncological processes is not provided. From the data presented in the table, it can be seen that high titers of cancer-risk strains of viruses such as HPV – 16, HPV – 18, HPV – 42 were detected in patients with vaginal cancer, which requires the search for drugs. For the pathogenetic treatment of genital cancer. The somatic condition of women with vaginal cancer did not differ from the somatic health of women with cancer in other places. Most often, patients with vaginal cancer suffer from obesity, inflammatory diseases of the urinary system (chronic pyelonephritis, cystitis) and chronic obstructive pulmonary diseases.

### References

- Zhang, Q. et al. Oncologic and obstetrical outcomes with fertility-sparing treatment of cervical cancer: a systematic review and meta-analysis // *Oncotarget*. 2017.– T. 8.
- Datta, N. R., Stutz, E., Gomez, S., & Bodis, S. (2018). Efficacy and safety evaluation of the various therapeutic options in locally advanced cervix cancer: A systematic review and network meta-analysis of randomized clinical trials. *International Journal of Radiation Oncology\* Biology\* Physics*. Doi:10.1016/j.ijrobp.2018.09.037
- Nagy, V. M. et al. Randomized phase 3 trial comparing 2 cisplatin dose schedules in 326 patients with locally advanced squamous cell cervical carcinoma: long-term follow-up // *International Journal of Gynecologic Cancer*. 2012.– T. 22.– № 9.



- Duenas-González, A. et al. Phase III, open-label, randomized study comparing concurrent gemcitabine plus cisplatin and radiation followed by adjuvant gemcitabine and cisplatin versus concurrent cisplatin and radiation in patients with stage IIB to IVA carcinoma of the cervix // *Journal of Clinical Oncology*. 2011. – T. 29. – P. 13.
- Mabuchi, S. et al. Chemoradiotherapy followed by consolidation chemotherapy involving paclitaxel and carboplatin and in FIGO stage IIIB/IVA cervical cancer patients. / *J Gynecol Oncol*. 2017. Jan; 28(1): e15. Doi: 10.3802/jgo.2017.28.e15
- Wang, S. et al. Efficacy of concurrent chemoradiotherapy plus adjuvant chemotherapy on advanced cervical cancer / *Chin J Cancer*. 2010. Nov; 29 (11): 59–63.
- Narayan, S. et al. Pros and cons of adding of neoadjuvant chemotherapy to standard concurrent chemoradiotherapy in cervical cancer: a regional cancer center experience // *The Journal of Obstetrics and Gynecology of India*. 2016. – T. 66. – № 5. – P. 385.
- Cella, D. et al. Health-related quality of life outcomes associated with four cisplatin-based doublet chemotherapy regimens for stage IVB recurrent or persistent cervical cancer: a Gynecologic Oncology Group study // *Gynecologic oncology*. 2010. – T.
- Bjurberg, M. et al. Primary treatment patterns and survival of cervical cancer in Sweden: A population-based Swedish Gynecologic Cancer Group Study // *Gynecologic oncology*. 2019. – T. 155. – № 2. – P. 229–236.
- Sapienza, L. G. et al. Decrease in uterine perforations with ultrasound image-guided applicator insertion in intracavitary brachytherapy for cervical cancer: A systematic review and meta-analysis // *Gynecologic oncology*. 2018. – T. 151. – № 3. – P. 573.
- Zhang, J. et al. Diagnostic significance of magnetic resonance imaging in patients with cervical cancer after brachytherapy: a meta-analysis // *Acta Radiologica*. 2019.
- Barillot, I. et al. Carcinoma of the cervical stump: a review of 213 cases // *European Journal of Cancer*. 1993. – T. 29. – № 9. – P. 1231–1236.
- Chen, X., Zou, H., Li, H., Lin, R., Su, M., Zhang, W., ... Zou, C. (2017). Weekly Versus Triweekly Cisplatin-Based Chemotherapy Concurrent With Radiotherapy in the Treatment of Cervical Cancer. *International Journal of Gynecological Cancer*, – 27(2).
- Kim, H.S. et al. Efficacy of neoadjuvant chemotherapy in patients with FIGO stage IB1 to IIA cervical cancer: an international collaborative meta-analysis // *European Journal of Surgical Oncology (EJSO)*. 2013. – T. 39. – № 2. – C. 115–124.
- Penson, R.T. et al. Patient Reported Outcomes in a Practice Changing Randomized Trial of Bevacizumab in the Treatment of Advanced Cervical Cancer: An NRG Oncology/ Gynecologic Oncology Group Study // *The Lancet. Oncology*. 2015. – T.
- Kitagawa, R. et al. A multi-institutional phase II trial of paclitaxel and carboplatin in the treatment of advanced or recurrent cervical cancer // *Gynecologic oncology*. 2012. – T. 125. – № 2. – P. 307–311.
- Tewari, K.S. et al. Bevacizumab for advanced cervical cancer: final overall survival and adverse event analysis of a randomised, controlled, open-label, phase 3 trial (Gynecologic Oncology Group 240) // *The Lancet*. 2017. – T. 390. – № 10103. – P. 1654–1663.
- Friedlander, M., Grogan M. Guidelines for the treatment of recurrent and metastatic cervical cancer // *The oncologist*. 2002. – T. 7. – № 4. – P. 342–347.
- Poorolajal, J., Jenabi E. The association between BMI and cervical cancer risk: a metaanalysis // *European Journal of Cancer Prevention*. 2016. – T. 25. – № 3. – P. 232–238.

submitted 22.08.2024;

accepted for publication 20.09.2024;

published 8.10.2024

© Polatova, D. Sh., Artikhodzhaeva, G. Sh.

Contact: yuldashkhodjaevanigina@gmail.com



## Section 3. Technical ingeneral

DOI:10.29013/EJTNS-24-1-16-29



### EARTHQUAKE PREDICTION USING SHORT RADIOWAVE TECHNOLOGY

**Khaladdin Javadov <sup>1</sup>**

<sup>1</sup> Engineer, Azerbaijan

---

**Cite:** Javadov Kh. (2024). *Earthquake Prediction Using Short Radiowave Technology*. *European Journal of Technical and Natural Sciences* 2024, No 1. <https://doi.org/10.29013/EJTNS-24-1-16-29>

---

#### Abstract

An earthquake prediction must define 3 elements: 1) the date and time, 2) the location, and 3) the magnitude. Yes, some people say they can predict earthquakes, but here are the reasons why their statements are false: They are not based on scientific evidence, and earthquakes are part of a scientific process. Earthquake prediction is a branch of the science of seismology concerned with the specification of the time, location, and magnitude of future earthquakes within stated limits, and particularly “the determination of parameters for the next strong earthquake to occur in a region”. An earthquake is the shifting of the Earth’s plates, which results in a sudden shaking of the ground that can last for a few seconds to a few minutes. Within seconds, mild initial shaking can strengthen and become violent. Earthquakes happen without warning and can happen at any time of year.

**Keywords:** *Earthquake, Radio wave, microwave, X-ray, visible light, Transmitter, Receiver, Electromagnetic Field*

#### Introduction

They are both signs of seismic movement within the earth. The difference is the intensity of the movement. Earthquakes are more intense than earth tremors. When a tremor exceeds five on the moment magnitude scale — a scale between 0 to 10 — then. There are four different types of earthquakes: tectonic, volcanic, collapse and explosion. The magnitude scale is logarithmic. This means that, at the same distance, an earthquake of magnitude 6 produces vibrations with am-

plitudes 10 times greater than those from a magnitude 5 earthquake and 100 times greater than those from a magnitude 4 earthquake. A few people may get unlucky and have objects fall on them, but modern well-built buildings should have no difficulty riding out magnitude 6 quakes. In areas that build using load-bearing masonry or use a lot of masonry cladding, a magnitude 6 quake is enough to cause significant damage and may cause some deaths. Megathrust earthquakes occur at convergent plate boundaries, where

one tectonic plate is forced underneath another. The earthquakes are caused by slip along the thrust fault that forms the contact between the two plates. These interplate earthquakes are the planet's most powerful, with moment magnitudes ( $M_w$ ) that can exceed 9.0. Since 1900, all earthquakes of magnitude 9.0 or greater have been megathrust earthquakes. The thrust faults responsible

for megathrust earthquakes often lie at the bottom of oceanic trenches; in such cases, the earthquakes can abruptly displace the sea floor over a large area. As a result, megathrust earthquakes often generate tsunamis that are considerably more destructive than the earthquakes themselves. Teletsunamis can cross ocean basins to devastate areas far from the original earthquake.

**Figure 1.** Terminology and mechanism

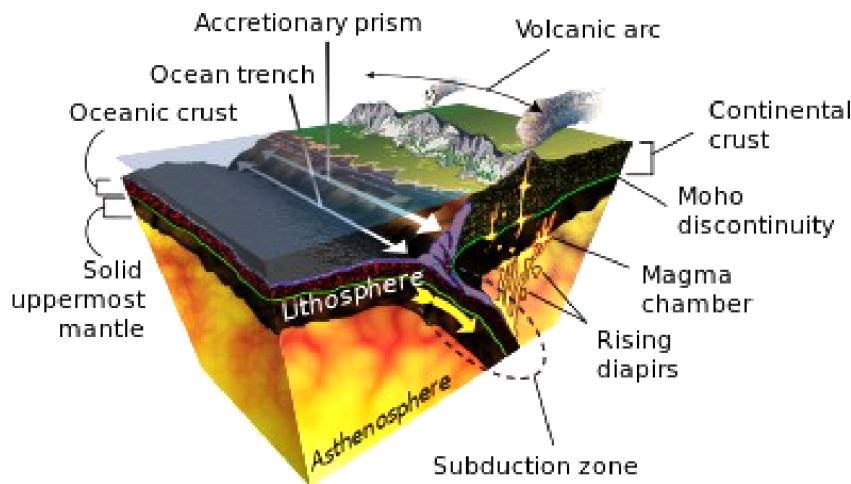
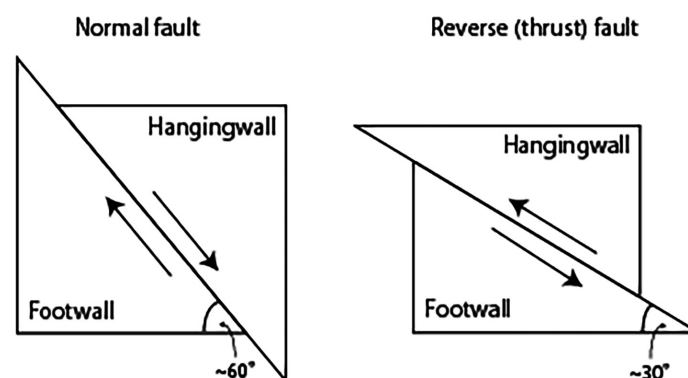


Diagram of a subduction zone. The megathrust fault lies on the top of the subducting slab where it is in contact with the overriding plate. The term *megathrust* refers to an extremely large thrust fault, typically formed at the plate interface along a

subduction zone, such as the Sunda megathrust. However, the term is also occasionally applied to large thrust faults in continental collision zones, such as the Himalayan megathrust. A megathrust fault can be 1.000 kilometers (600 mi) long.

**Figure 2.** Cross-sectional illustration of normal and reverse faults



A thrust fault is a type of reverse fault, in which the rock above the fault is displaced upwards relative to the rock below the fault. This distinguishes reverse faults from normal faults, where the rock above the fault is displaced downwards, or strike-slip faults, where the rock on one side of the fault is dis-

placed horizontally with respect to the other side. Thrust faults are distinguished from other reverse faults because they dip at a relatively shallow angle, typically less than 45°, and show large displacements. In effect, the rocks above the fault have been thrust over the rocks below the fault. Thrust faults

are characteristic of areas where the Earth's crust is being compressed by tectonic forces. Megathrust faults occur where two tectonic plates collide. When one of the plates is composed of oceanic lithosphere, it dives beneath the other plate (called the *overriding plate*) and sinks into the Earth's mantle as a *slab*. The contact between the colliding plates is the megathrust fault, where the rock of the overriding plate is displaced upwards relative to the rock of the descending slab. Friction along the megathrust fault can lock the plates together, and the subduction forces then build up strain in the two plates. A megathrust earthquake takes place when the fault ruptures, allowing the plates to abruptly move past each other to release the accumulated strain energy.

### Occurrence and characteristics

Megathrust earthquakes are almost exclusive to tectonic subduction zones and are often associated with the Pacific and Indian Oceans. These subduction zones are not only responsible for megathrust earthquakes but are also largely responsible for the volcanic activity associated with the Pacific Ring of Fire. Since the earthquakes associated with these subduction zones deform the ocean floor, they often generate a significant series of tsunami waves. Subduction zone earthquakes are also known to produce intense shaking and ground movements for significant periods of time that can last for up to 3–5 minutes. In the Indian Ocean region, the Sunda megathrust is located where the Indo-Australian Plate is subducting under the Eurasian Plate and extends 5.500 kilometres (3.400 mi) off the coasts of Myanmar, Sumatra, Java and Bali before terminating off the northwestern coast of Australia. This subduction zone was responsible for the 2004 Indian Ocean earthquake and tsunami. In Japan, the Nankai megathrust under the Nankai Trough is responsible for Nankai megathrust earthquakes and associated tsunamis. In North America, the Juan de Fuca Plate is subducting under the North American Plate creating the Cascadia subduction zone which stretches from mid Vancouver Island, British Columbia to Northern California. This subduction zone was responsible for the 1700 Cascadia earthquake. The Aleutian Trench, of the southern coast of

Alaska, and the Aleutian Islands, where the North American Plate overrides the Pacific Plate, has generated many major earthquakes throughout history, several of which generated Pacific-wide tsunamis, including the 1964 Alaska earthquake; at magnitude 9.2, it remains the largest recorded earthquake in North America, and the second-largest earthquake instrumentally recorded in the world. The largest recorded megathrust earthquake was the 1960 Valdivia earthquake, estimated magnitude 9.5, centered off the coast of Chile along the Peru-Chile trench, where the Nazca Plate is subducting under the South American Plate. This megathrust region has regularly generated extremely large earthquakes. The largest megathrust event within the last 20 years was the magnitude 9.1 Tōhoku earthquake.<sup>1</sup> The largest possible earthquake that is estimated to occur is a magnitude 10, with some scientists even estimating that a magnitude 11 earthquake could occur, though extremely rare. Where they would take place is most likely to be a combined rupture of the Japan Trench and Kuril-Kamchatka Trench. A study reported in 2016 found that the largest megathrust quakes are associated with down-going slabs with the shallowest dip, so-called flat slab subduction. Compared with other earthquakes of similar magnitude, megathrust earthquakes have a longer duration and slower rupture velocities. The largest megathrust earthquakes occur in subduction zones with thick sediments, which may allow a fault rupture to propagate for great distances unimpeded.

*Prior to large earthquakes the Earth sends out transient signals, sometimes strong, more often subtle and fleeting. These signals may consist of local magnetic field variations, electromagnetic emissions over a wide range of frequencies, a variety of atmospheric and ionospheric phenomena.*

What happens to the Earth before an earthquake? Before an earthquake, the buildup of stress in the rocks on either side of a fault results in gradual deformation. Eventually, this deformation exceeds the frictional force holding the rocks together and sudden slip occurs along the fault. The tectonic plates are always slowly moving, but they get stuck at their edges due to friction. When the stress on the edge overcomes the friction, there is



an earthquake that releases energy in waves that travel through the earth's crust and cause the shaking that we feel. According to the US Geological Survey, computer models by Richard Gross (Jet Propulsion Laboratory) indicate that the quake shifted the continental plates enough to speed up the planet's spin (through the conservation of angular momentum) by some 0.0000027 second per day.

Perhaps no seismic subject is as irksome to seismologists as discussions of earthquake size. There often seems to be no end of confusion, misunderstanding, and over-interpretation of what are really pretty crude metrics. And when news announcers mention the "Richter Scale" seismologists the world over begin gnashing their teeth.

### **Magnitude**

A familiar analogy to help understand earthquake size metrics is to think about a light bulb. One measure of the strength of a light bulb is how much energy it uses. A 100-watt bulb is brighter than a 50-watt bulb, but not nearly as bright as a 250-watt bulb. The wattage of a bulb tells you about the strength of the light source. In the same way, an earthquake's *magnitude* is an objective measurement of the energy radiated by an earthquake. However, earthquake magnitude has no physical units, nor a meaningful 0. This is because we can't easily measure the energy the way we can with an electric circuit, so seismologists commonly use a relative measure. It is easier to choose a particular earthquake recorded at a particular distance as a "standard" earthquake and call it a magnitude 1. An earthquake that causes ground motion at a seismic station (when corrected for distance) 10 times larger than the reference earthquake is M2. An earthquake causing motion at that distance 10 times larger than an M2 is an M3, and so on. To achieve this ten fold increase in ground motion requires about 32 to 33 times the energy. When referring to the power or energy released in an earthquake this 32 multiplier is used. An earthquake that releases about 33 times less energy and causes motion 10 times smaller than an M1 is an M0—and magnitudes can even go negative.

### **Intensity**

Earthquake *intensity* measures how strongly the earthquake impacts a specific location. In the light bulb analogy, it is the brightness with which you perceive the light at a place in a room. Can you read a fine-print book by the lamp? Pick up a needle? Perform delicate surgery? Depends on the wattage of the bulb, and how far you are from it, right? If you mapped out the brightness in terms of what you could accomplish at the light level in a room, you'd have an intensity map.

Well, you can make a map of earthquake impacts using the Modified Mercalli Intensity Scale (MMI), which derived from an earlier ten-degree Rossi-Forel scale, later revised by Italian volcanologist Giuseppe Mercalli in 1884 and 1906 to quantify (somewhat) the earthquake's effects. Further refinements for more modern construction were published in 1931 by the American seismologists Harry Wood and Frank Neumann. Measurements of intensity using the Modified Mercalli scale, are composed of 12 increasing levels that range from imperceptible shaking to catastrophic destruction, usually designated by Roman numerals, which stresses their semi-quantitative nature. Whereas an earthquake will have one magnitude (well, as noted below, there are likely to be several different estimates of the magnitude of an earthquake depending on the type of estimate etc.), for each individual earthquake there will be a range of intensities depending in part on the magnitude of the source, but also the location of the site at which the intensity was observed.

### **More about Magnitudes – The 3 Approaches**

If you've had some time to think a bit about the Earthquake/Light bulb analogy you probably have come up with some questions, like: But some bulbs are blue and some white and some yellow, what gives with that? And, fluorescent fixtures put out really different quality light than incandescents, and are brighter for the same wattage, eh? And, what about a flash bulb from my camera which is incredibly bright...but just for a fraction of second? And, if my room is filled with steam or smoke, is the intensity still the same? These are all good points; it turns out that simi-

larly for earthquakes the complexities and variability of earthquake rupture processes and of seismic waves as they travel through Earth (and evolving seismometer design and sensitivities) there are different methods for measuring the magnitude of an earthquake. These may return a slightly different number when used to estimate the energy released in an earthquake. In overview, there are three approaches to using seismograph recordings to quantify earthquake sizes, with numerous flavors of each. One approach is to use some measure of peak amplitudes recorded on seismograms. A second is to use the duration of shaking recorded. A third is to try to match the actual waveform wiggle-for-wiggle with a mathematical model (a “synthetic seismogram”), and report the size of the modeled earthquake.

#### ***Amplitude based Magnitudes (Local, Body Wave, Surface Wave)***

The oldest and most famous magnitude measurement method, the *Local Magnitude* (it used to be referred to as the Richter magnitude), was developed by Dr. Charles Richter and Beno Gutenberg of Cal Tech in 1935. Written as  $M_L$ , it remains the go-to method for measuring small- to medium-sized earthquakes within 600 km from the recording seismograph. Richter used seismograms recorded on a particular instrument, the Wood-Anderson torsion seismograph. Today, we use more modern instruments and account for their response to mimic what the historical Wood-Anderson seismograph would have produced. Richter’s motivation for creating the local magnitude scale was to measure the ratio of small- to medium-sized earthquakes. It was never intended to measure large or distant earthquakes. All amplitude-based magnitudes rely on a base-10 logarithm of the peak amplitude measured by a seismograph. This is because there are many factors of 10 difference between the smallest and largest amplitudes of observed ground motions. An earthquake that measures 5.0 on the Richter scale has a shaking amplitude 10 times larger and corresponds to an energy release of 31.6 times greater than one that measures 4.0.

*Body wave magnitude* is a similar concept, but applied usually to teleseisms – earthquakes more than 3000 km from the

recording station – and good for deep and shallow earthquakes.

*Surface wave magnitudes* measure the surface waves that are generated by large regional to teleseismic earthquakes, and that travel long distances without losing much energy from absorption.

In general local magnitudes “saturate” (lose resolution) for earthquakes exceeding  $M_{5.8}$  or so, body waves stay on scale to somewhat larger magnitudes, while surface wave magnitudes saturates at about  $M_8$  or so. This is in general because of the frequencies of the seismic waves that each use. The higher-frequency methods (local, duration) can’t see the difference between larger earthquakes, while the low frequency measures (surface waves, moment magnitude) characterize the long-wavelength energy that radiates from a bigger rupture surface.

#### ***Duration Magnitudes (coda magnitude)***

Another estimate of magnitudes is particularly useful when recordings “clip” and you can’t measure the peak amplitude. This is called the coda magnitude, or duration magnitude, and is derived from the observation that the ratio of peak amplitude to the duration of shaking from an earthquake are related. PNSN often calculates the size of PNW earthquakes using the durations averaged from a number of seismograms to obtain “ $M_d$ ” estimates. In the past a seismic analyst picked the duration on each seismogram by eye independently, which was somewhat subjective and variable, as the background noise varies greatly. The modern method, made possible by faster computers, is to model the decaying amplitude of the seismogram in order to automatically and objectively define a duration.

#### ***Waveform Modeling (moment magnitude)***

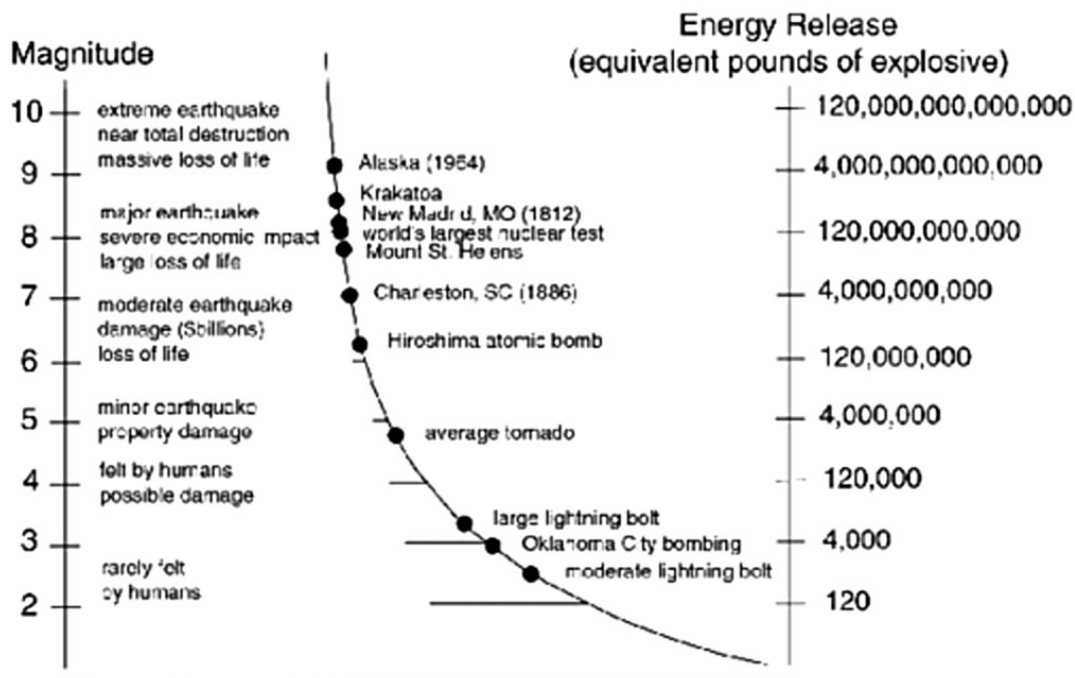
Modern digital seismic instrumentation, modern seismic theory, and most of all modern high-speed computers have permitted us to be able to model seismograms wiggle-for-wiggle. To do this, we use a standard model of the Earth and of the source to generate synthetic seismograms, and the computer adjusts the location, size, and orientation of the rupture to match the observed waveforms. The magnitude that is derived from waveform modeling is called the *Mo-*

ment magnitude, and it is in some ways the most precise estimate of earthquake size – and the only one applicable to great earthquakes  $M > 8$ . Of great interest is that since we can observe the deformation of the Earth from such big earthquake ruptures, we have an independent estimate of the energy they released, so that we can (finally!) relate the magnitude to the energy released during rupture. It is worthwhile to note that all of these approaches have been calibrated and defined with respect to each other such that they all agree, on average, in the ranges in which they overlap. So for general purposes an M8 is an M8, regardless of the method that

generated it. But also it is interesting that Richter's original local magnitude was the one that all the other techniques generally matched up with (since it was first) so, in a sense, the "Richter Scale" that news reporters often cite (to the chagrin of us seismologists) is really a pretty apt homage.

Below is a representation, from the Geological Society of America, of earthquake magnitudes and the equivalent energy release. (For the life of us, we don't know why the geologists used pounds of explosive as a proxy for energy instead of a real physical unit of energy, such as Joules! But the figure makes the point, anyway.)

**Figure 3.** Richter Scale



### Magnitude and Energy

Notice the relationship is not linear? The change in the amount of energy released from one magnitude to the next is greater as the earthquake magnitude increases. For example, the difference in amount of energy released from a magnitude 5 to a magnitude 10 is not double, it is 30 million times as much!

Need some further practice relating Earthquake Magnitude to Energy? No problem, the USGS calculates the difference between a 5.8 and 8.7 earthquake and has a calculator where you can input your own numbers to see how much bigger an earthquake can get with different magnitudes.

### Magnitude Vs. Intensity

The chart below claims to compare Richter Scale magnitudes with intensities in a very generalized way – as if a "Richter magnitude" was somehow measuring the same thing as a "Mercalli intensity". Now that you know the basics of earthquake Magnitudes and earthquake Intensities, you know that this chart makes no sense. If you see it or a similar representation, you can be assured the provider of the information is unencumbered by knowledge of the basics.



**Figure 4.** Mercalli vs Richter Scale (2)

Rich ter	Mercalli	Earthquake Effects
2	I	<b>Instrumental.</b> Not felt except by a very few under especially favourable conditions detected mostly by Seismography.
	II	<b>Feeble.</b> Felt only by a few persons at rest, especially on upper floors of buildings.
	III	<b>Slight.</b> Felt quite noticeably by persons indoors, especially on upper floors of buildings. Many people do not recognize it as an earthquake. Standing motor cars may rock slightly. Vibration similar to the passing of a truck.
3	IV	<b>Moderate.</b> Felt indoors by many, outdoors by few during the day. At night, some awakening. Dishes, windows, doors disturbed; walls make cracking sound. Sensation like a heavy truck striking building. Standing motor cars rock noticeably.
4	V	<b>Rather Strong.</b> Felt by nearly everyone; many awakened. Some dishes, windows broken. Un-stable objects overturned. Pendulum clocks may stop.
5	VI	<b>Strong.</b> Felt by all, many frightened. Some heavy furniture moved; a few instances of fallen plaster. Damage slight.
	VII	<b>Very Strong.</b> Damage negligible in buildings of good design and construction; slight to moderate in well-built ordinary structures; considerable damage in ordinary structures; considerable damage in poorly built or badly designed structures.
6	VIII	<b>Destructive.</b> Damage slight in specially designed structures; considerable damage in ordinary substantial buildings with partial collapse. Damage great in poorly built structures. Fall of factory stacks, columns, monuments, walls. Heavy furniture overturned.
7	IX	<b>Ruinous.</b> Damage considerable in specially designed structures; well designed frame structures thrown out of plumb. Damage great in substantial buildings, with partial collapse. Buildings shifted off foundations.
	X	<b>Disastrous.</b> Some well-built wooden structures destroyed; most masonry and frame structures destroyed with foundations. Rails bend greatly.
8	XI	<b>Very Disastrous.</b> Few, if any (masonry) structures remain standing. Bridges destroyed. Rails bend greatly.
	XII	<b>Catastrophic.</b> Damage total. Lines of sight and level are distorted. Objects thrown into the air.

### One Final Word – a Plea for Understanding

Now that you know how many different approaches there are to measuring an earthquake, and how it depends on the traces that you use, and instrument types that you have available and how far they are from the earthquake, and how many there are...

Perhaps you'll understand why our magnitude estimates change with time immedi-

ately after an earthquake as we try to be both as fast and as accurate as possible. And why different organizations will post somewhat different magnitudes for the same earthquake.

A rule of thumb, perhaps, is that in the early minutes (or tens of minutes) after an earthquake up to a half a magnitude unit of difference between estimates will generally be shrugged off by seismologists as reason-

able scatter. But differences larger than that usually mean that there was a fairly serious problem...like the entirely wrong technique was used, or critical data were omitted.

### ***Is there a magnetic field before an earthquake?***

Electromagnetic variations have been observed after earthquakes, but despite decades of work, there is no convincing evidence of electromagnetic precursors to earthquakes.

What are the electromagnetic fields of earthquakes?

Seismo-electromagnetics are various electro-magnetic phenomena believed to be generated by tectonic forces acting on the Earth's crust, and possibly associated with seismic activity such as earthquakes and volcanoes.

How does electromagnetic energy change?

### **ELECTROMAGNETIC WAVES**

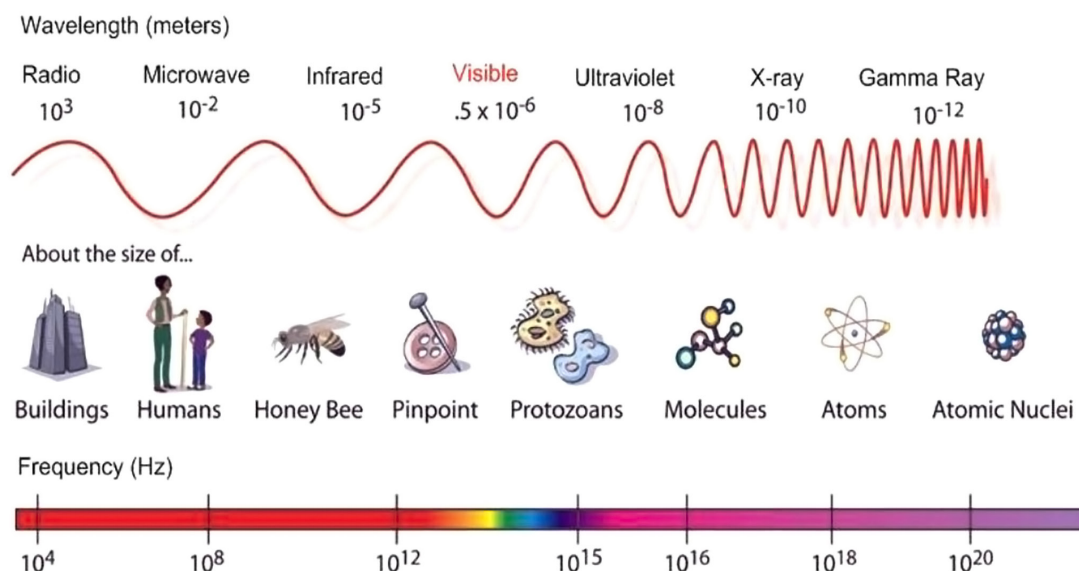
A changing magnetic field will induce a changing electric field and vice-versa – the two are linked. These changing fields form electromagnetic waves. Electromagnetic waves differ from mechanical waves in that they do not require a medium to propagate.

What causes electromagnetic fields?

They are generated by natural phenomena like the Earth's magnetic field but also by human activities, mainly through the use of electricity. Mobile phones, power lines and computer screens are examples of equipment that generates electromagnetic fields.

What are the 7 types of electromagnetic waves?

**Figure 5.**



There are seven types of electromagnetic waves: radio waves, microwaves, infrared light, visible light, ultraviolet light, X-rays, and gamma rays.

## **Chapter 2. Electromagnetic Fields Generated by Earthquakes**

### ***Introduction***

*Independent knowledge of the physical processes that occur with seismic events can be obtained from observations of electric and magnetic fields generated by these complex processes. During the past few decades, we have seen a remarkable increase in the quality and quantity of electromagnetic (EM) data recorded before and during*

*earthquakes and volcanic eruptions. This paper describes the most significant recent data and the implications these data have for different generating mechanisms. We note that, despite several decades of relatively high quality monitoring, clear demonstration of the existence of precursory EM signals has not been achieved, although causal relations between coseismic magnetic field changes and earthquake stress drops are no longer in question. This paper extends discussions of tectonomagnetism and tectonoelectricity, over the various parts of the electromagnetic spectrum from radio frequencies (RF) to submicrohertz frequencies.*

### ***Statement of the Problem***

This chapter reviews recent results of magnetic, electric, and electromagnetic disturbances apparently associated with earthquakes and discusses the physical mechanisms likely to have produced them. Although some observations are larger than expected, the best field observations are generally in agreement with calculations. Some observations are suggested as precursors yet have no corresponding co-event signals and some have co-event signals yet no precursory signals.

### ***Summary of Physical Mechanisms Involved***

The loading and rupture of water-saturated crustal rocks during earthquakes, together with fluid/gas movement, stress redistribution, and change in material properties, has long been expected to generate associated magnetic and electric field perturbations. The detection of related perturbations prior to fault rupture has thus been proposed frequently as a simple and inexpensive method to monitor the state of crustal stress and perhaps to provide tools for predicting crustal failure.

### ***Basic Measurement Limitations***

The precision of local magnetic and electric field measurements on active faults varies as a function of frequency, spatial scale, instrument type, and site location. Most measurement systems on the Earth's surface are limited more by noise generated by ionosphere, magnetosphere, and by cultural noise than by instrumental noise. Thus, systems for quantifying these noise sources are of crucial importance if changes in electromagnetic fields are to be uniquely identified.

### ***Recent Results***

Although both electric and magnetic fields are expected to accompany dynamic physical processes in the Earth's crust, simultaneous measurements of both fields are not routinely made. I will therefore discuss separately, electric fields, magnetic fields, and electromagnetic fields during and preceding earthquakes. Magnetic and electric fields generated by earthquakes are termed "seismomagnetic (SM)" and "seismoelectric (SE)" effects. Those preceding earthquakes, or occurring at other times, are and now How can we predict the earthquake.

### ***Can we feel Earth's magnetic field?***

A new study hints that humans have magnetoreception abilities, similar to some other animals. ANIMAL MAGNETISM Like birds, bacteria and other creatures with an ability known as magnetoreception, humans can sense Earth's magnetic field (illustrated), a new study suggests.

When did Earth have a magnetic field?

Earliest appearance. Paleomagnetic studies of Paleoproterozoic lava in Australia and conglomerate in South Africa have concluded that the magnetic field has been present since at least about 3,450 million years ago.

Can we feel electromagnetic fields?

Exposure to electric, magnetic and electromagnetic fields (EMF), if they are strong enough, can lead to short term health effects. Exposure to low frequency fields that are strong enough can lead to dizziness, seeing light flashes and feeling tingling or pain through stimulation of nerves.

Do earthquakes cause electromagnetic disturbances?

Earthquake taking place in a fluid-saturated porous medium can generate electromagnetic (EM) waves because of the electrokinetic effect.

Do tectonic plates cause magnetic field?

No. The tectonic plates are continually moving because of the convection currents in the mantle, which is a viscoelastic solid. The magnetic fields are generated by convection currents in the outer core, which is completely liquid.

What does frequency do to earthquakes?

The corner frequency is inversely correlated with magnitude. Therefore, small earthquakes have a proportionally greater content of high frequencies. Humans can hear sound waves mainly in the range of 20 to 20,000 Hz.

What frequency causes earthquakes?

0.2 Hz to 20 Hz

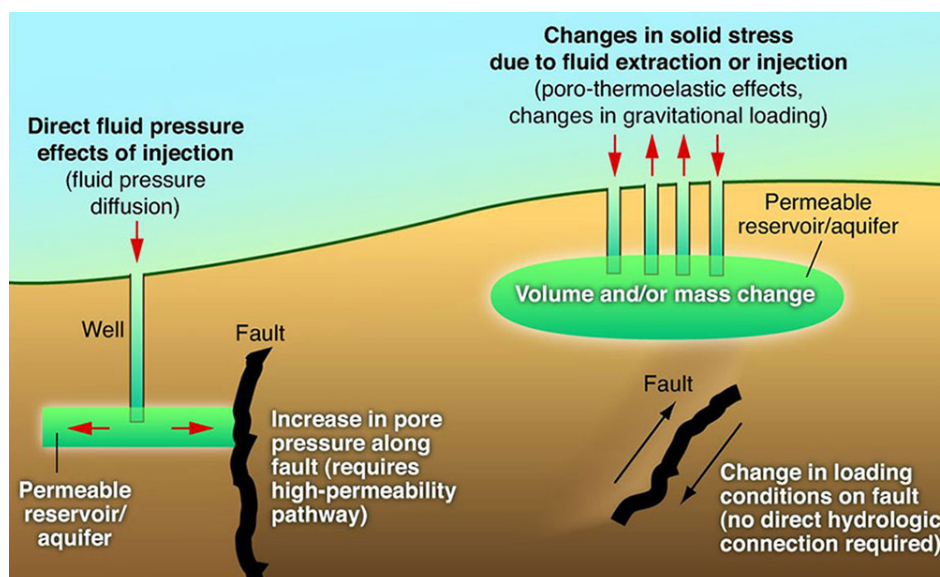
Earthquake Motion

The movement during fault rupture produces a range of vibrations, or seismic waves, that are radiated outwards. The vibrations of engineering significance occur at frequencies from less than 0.2 Hz to 20 Hz (periods from about 5 seconds down to about 0.05 seconds).

Can earthquakes be triggered artificially?



**Figure 6.**



Injecting liquids into waste disposal wells, most commonly in disposing of produced water from oil and natural gas wells, has been known to cause earthquakes. This high-saline water is usually pumped into salt water disposal (SWD) wells.

So we start, the frequency of earth is 11.79 Hz.

The earth's magnetic field has a frequency of 11.79 Hz (cycles per second). There is also a second frequency within the earth's ionosphere called the Schumann Resonance,

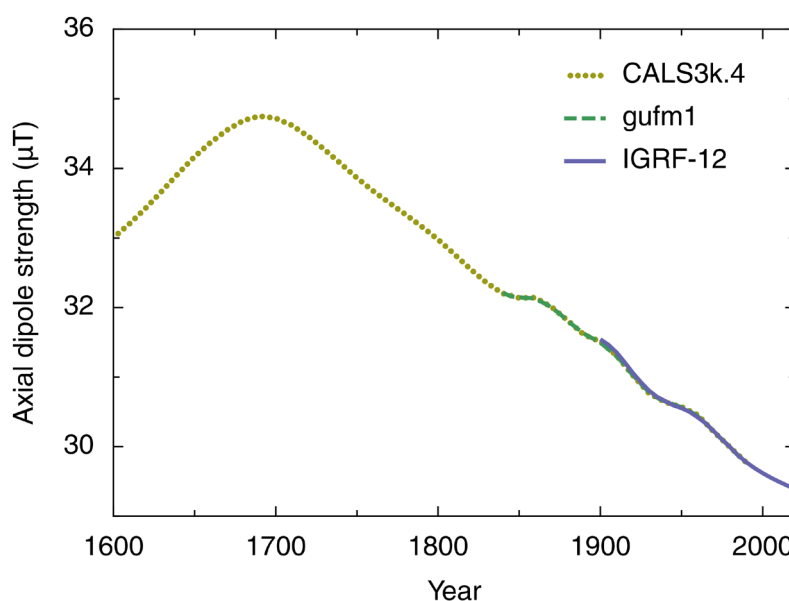
which resonates at 7.83 Hz. This frequency is created mainly by lightning strikes... approximately 7 million per day.

What frequency is a magnetic field?

The magnitude (intensity) of a magnetic field is usually measured in Tesla (T or mT). Static magnetic fields do not vary over time, and as such do not have a frequency (0 Hz). Examples are the fields generated by a permanent magnet or the Earth's magnetic field.

What is the magnetic field constant of the Earth?

**Figure 7.**



The Earth's field ranges between approximately 25 and 65  $\mu\text{T}$  (0.25 and 0.65 G). By

comparison, a strong refrigerator magnet has a field of about 10,000  $\mu\text{T}$  (100 G). A map of

intensity contours is called an isodynamic chart.

I got this from my grade 12 physics notes. It says that Earth, having a mass of  $6.0 \times 10^{25}$  kg and a speed of  $3.0 \times 10^4$  m/s, when plugged into the wavelength equation  $\lambda = h/(mu)$  (where  $u$  is speed), has a wavelength of  $4 \times 10^{-63}$  m. Then, does this mean it has a frequency of  $7.5 \times 10^{70}$  Hz? If so, then it also means that the Earth's wave's energy is  $4.97 \times 10^{37}$  J. My main confusion is that I always hear scientists say that quantum mechanics has practically no effect on the macroscopic world (except for some things like bucky balls and superconductors). I would think that a wave with the energy of  $4.97 \times 10^{37}$  J would have to have an enormous effect on something or even the Earth in an interference pattern using the Sun and other planets as its own really large double slit experiment.

Shortwave radio frequency energy is capable of reaching any location on the Earth as it is influenced by ionospheric reflection back to the earth by the ionosphere, (a phenomenon known as "skywave propagation"). A typical phenomenon of shortwave propagation is the occurrence of a skip zone where reception fails.

What frequency is short wave?

How far can radio waves travel through the ground?

The range of the ground wave (up to 1.600 km [1.000 miles]) and the bending and reflection of the sky wave by the ionosphere depend on the frequency of the waves. Under normal ionospheric conditions 40 MHz is the highest-frequency radio wave that can be reflected from the ionosphere.

How far can radio waves travel from Earth?

Ground stations can communicate with satellites and spacecraft billions of miles from Earth.

Can microwaves reach Earth?

Microwaves have a long wavelength, though not as long as radio waves. The Earth's atmosphere is transparent to some wavelengths of microwave radiation, but not to others. The longer wavelengths (waves more similar to radio waves) pass through the Earth's atmosphere more easily than the shorter wavelength microwaves.

We all want good, stable and reliable communication. Some make certain sacrifices for this, drilling into the roofs of their iron horses, cutting in powerful antennas, installing expensive stations, amplifiers, and doing their best to raise the class of communication equipment in order to provide themselves with this very connection. However, for some reason, everyone forgets about such a subtle thing as the ether, in which, in fact, radio waves propagate, and whether you can establish contact with the correspondent you are interested in or not depends 100% on the "mood" of this very ether. We need to start with the fact that Ether and its state is a spontaneous phenomenon and does not depend on our desires and aspirations. Everything that happens on the air is subject to the strict laws of physics and we are unable to influence one or another aspect of the passage of radio waves through space. You just need to accept this, just like accepting that gravity exists on earth, and apples from an apple tree will always fall to the ground and not fly into space.

Why can shortwave radio signals go worldwide?

Shortwave radio frequency energy is capable of reaching any location on the Earth as it is influenced by ionospheric reflection back to the earth by the ionosphere, (a phenomenon known as "skywave propagation"). What I found from the history, that prior to earthquake (appr. 2 hours before) magnetic field of the Earth is being changed, and it becomes more,, transparent,, for some radio frequencies' the 2 portable radio transmitters can communicate in the distance of 1.6 km maximum.

Shortwave radio received its name because the wavelengths in this band are shorter than 200 m (1.500 kHz) which marked the original upper limit of the medium frequency band first used for radio communications. The broadcast medium wave band now extends above the 200 m / 1.500 kHz limit.

What is this? Although it's always been controversial, the idea that the magnetic field may shift before earthquakes has been around for a while. The survey states that "despite decades of work, there is no convincing evidence of electromagnetic precursors to earthquakes."

Does the magnetic field change before an earthquake?

My answer is Yes. Recently, researchers who study the formation process of large and intermediate earthquakes have discovered that two to three days before the earthquake actually happens, there is a change in the local magnetic field. In theory, geological forces would already be at work, deforming the crust, even if in subtle ways.

Do earthquakes affect magnetism?

Earthquakes can affect magnetic fields on the Earth, but they do not necessarily do so. For example, if you have a bunch of magnets set up on a table and there is an earthquake, then the magnets may get knocked over or moved around.

What is a device detecting changes in the magnetosphere which precede an earthquake?

The present invention, a magnetometer, measures the change in the magnetosphere

that occurs before large seismic events and gives notice that an earthquake will occur shortly. A drop in the strength of magnetosphere occurs generally within a 24 hour period before a large quake.

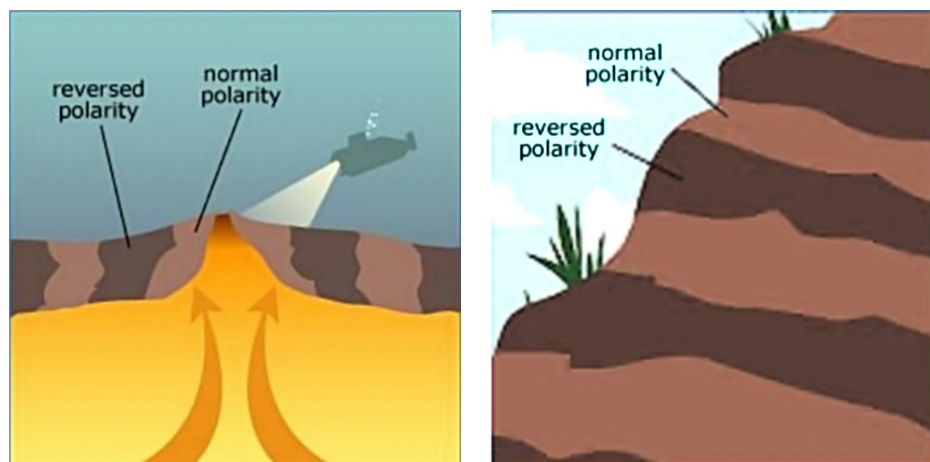
Please note that the magnetometer can predict with in 24 hours, monitoring with SHW technology will allow to predict the earthquake on earlier stages.

Do magnetic fields affect tectonic plates?

No. The tectonic plates are continually moving because of the convection currents in the mantle, which is a viscoelastic solid. The magnetic fields are generated by convection currents in the outer core, which is completely liquid. The magnetic field does not affect the convection currents in the mantle.

Does Earth's magnetic field affect plate tectonics?

**Figure 8.**



One of the key pieces of evidence supporting plate tectonic theory was the discovery that rocks on the seafloor record ancient reversals of the Earth's magnetic field: as rocks are formed where plates are moving away from one another, they record the current direction of the Earth's magnetic field, which flip-flops ...

Can the earthquake be man made?

Induced seismicity is typically earthquakes and tremors that are caused by human activity that alters the stresses and strains on Earth's crust. Most induced seismicity is of a low magnitude.

Can mankind create earthquakes?

Both the fracking process and wastewater disposal have been shown to trigger earthquakes. These aren't the only human activities that can trigger earthquakes, though.

Scientists point out that earthquakes can also be triggered by other human activities, such as construction of skyscrapers and nuclear explosions.

What device predicts earthquakes?

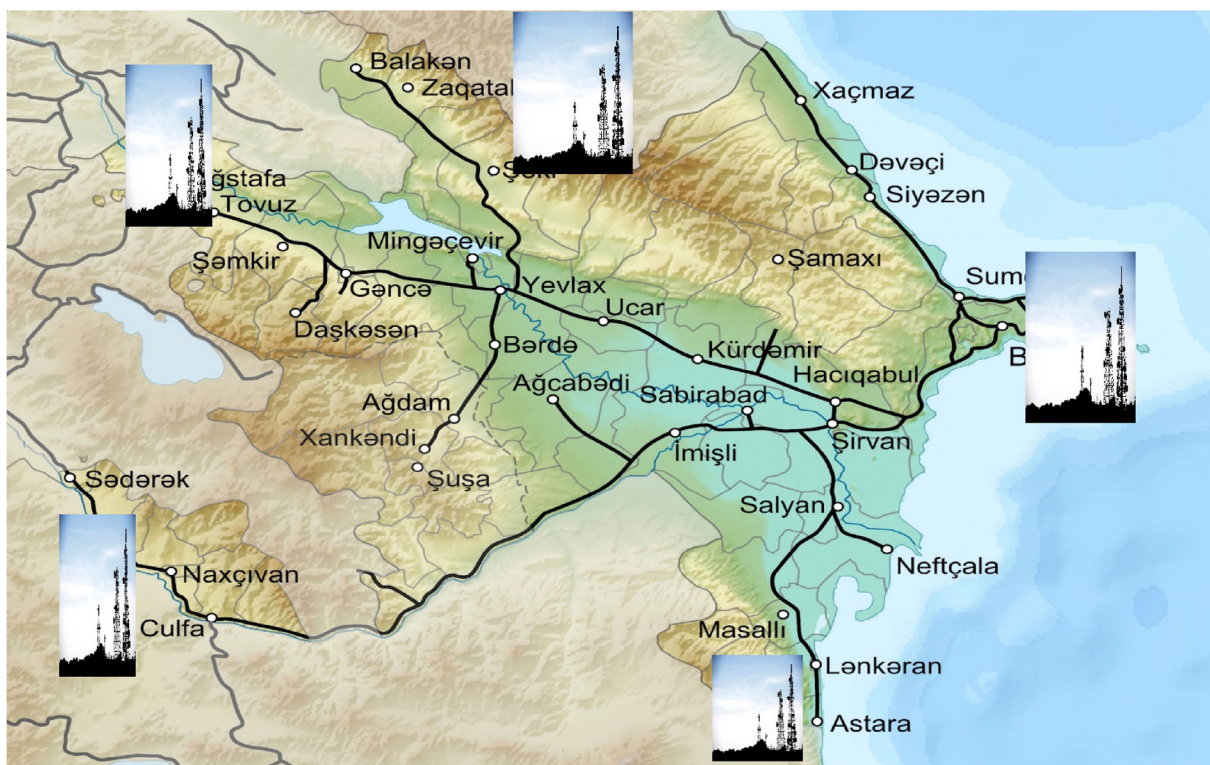
A seismograph or seismometer is the measuring instrument that creates the seismogram. Almost all seismometers are based on the principle of inertia, that is, where a suspended mass tends to remain still when the ground moves.

Can bombs cause earthquakes?

Even huge amounts of explosive almost never cause even small earthquakes, and it would take hundreds and thousands of small earthquakes to equal a large one, even if it could be done.



**Figure 10.**



Can phone detect earthquakes?

Each Android smartphone is equipped with tiny accelerometers that can act as mini seismometers. When a phone is plugged in and charging, it can detect the very beginnings of earthquake shaking.

What is the range of short radio waves?

3.000–30.000 kHz

Definition: Shortwave radio refers to radio broadcasts on a portion of the radio spectrum in the frequency range of 3.000–30.000 kHz (3–30 MHz).

I used the Azerbaijan map for instance just to explain the philosophy. We locate 5 portable radio stations in 5 different cities, Baku, Lenkoran, Nakhchivan, Tovuz, Balaken. And every transmitter/receiver will send a signal let's say every 2 minutes. In normal conditions

there will not be any changes, and no signals will be received due to long distance.

Also signal strength will be monitored continuously. Signal strength during transmitting/receiving is equal to 5mV (roughly) depends on station modification. But we can accept 5 mV.

And if we observe full signal receiving, or charging in MV, let's say between Baku and Tovuz, it will mean that there is a possibility of ground disturbance on that direction. Distance between Baku and Tovuz is 560km, having signal strength f.e. 2.5 mV, will mean that the possibility of ground disturbance on the middle of direction. This map can be extended and cities from neighbour countries can be added, f.e. from Turkey, Russia, Georgia etc.

## References

- USGS: Magnitude 8 and Greater Earthquakes Since 1900 Archived 2016-04-14 at the Wayback Machine.
- "Earthquakes with 50.000 or More Deaths Archived November 1, 2009, at the Wayback Machine". U.S. Geological Survey.
- Spence, William; S.A. Sipkin; G.L. Choy (1989). "Measuring the Size of an Earthquake". United States Geological Survey. Archived from the original on 2009-09-01. Retrieved 2006-11-03.



- “Instrumental California Earthquake Catalog”. WGCEP. Archived from the original on 2011–07–25. Retrieved 2011–07–24
- “USGS: Magnitude 8 and Greater Earthquakes Since 1900”. Archived from the original on April 14,
- “Historic Earthquakes and Earthquake Statistics: Where do earthquakes occur?”. United States Geological Survey. Archived from the original on 2006–09–25. Retrieved 2006–08–14.
- Fogler, Gillian R.; Wilson, Miles; Gluyas, Jon G.; Julian, Bruce R.; Davies, Richard J. (2018). “Global review of human-induced earthquakes”. *Earth-Science Reviews*. 178: 438–514
- Hough, Susan E.; Page, Morgan (2015). “A Century of Induced Earthquakes in Oklahoma?”. *Bulletin of the Seismological Society of America*. – 105 (6): 2863–2870. Bibcode:2015BuSSA.105.2863H. doi:10.1785/0120150109. Archived from the original on July 23, 2020. Retrieved July 23, 2020.
- “USGS Earthquake Magnitude Policy (implemented on January 18, 2002)”. Earthquake Hazards Program. USGS. Archived from the original on 2016–05–04. A copy can be found at “USGS Earthquake Magnitude Policy”. Archived from the original on 2017–07–3.

submitted 22.08.2024;  
accepted for publication 20.09.2024;  
published 8.10.2024  
© Javadov, Kh.  
Contact: Javadov2014@yahoo.co.uk



## Section 4. Transport

DOI:10.5281/zenodo.17724053



### THE FUTURE OF PORT LOGISTICS

**Pavlikhin Andrey**<sup>1</sup>

<sup>1</sup> Branch Manager, FS Mackenzie LLC, Novorossiysk, Russia

---

**Cite:** Pavlikhin, A. (2024). *The future of port logistics. European Journal of Technical and Natural Sciences 2024, No 1.* <https://doi.org/10.5281/zenodo.17724053>

---

#### Abstract

The article explores the key trends in digital transformation and automation of port logistics within the context of global and national sustainable development strategies. It examines modern models for integrating port management information systems and technologies that enhance productivity and environmental efficiency at terminals. Special attention is given to the role of Automated Guided Vehicles (AGVs) as a core element of technological modernization in ports. It is demonstrated that the combination of AGVs, Just-In-Time synchronization, Digital Twin technology, and robotics in STS cranes creates a new level of operational efficiency in ports. The article also analyzes the regulatory and environmental requirements set by IMO and the EU for the transition to smart and green ports. Predictive scenarios for phased automation in Russian ports are presented, and the prospects for implementing these solutions in the Black Sea and Baltic regions are outlined.

**Keywords:** *port logistics, maritime transportation, digitalization, automation, green ports, sustainable development, international trade, smart ports, innovation, transport infrastructure*

#### Introduction

Global maritime trade and port logistics continue to be fundamental components of global supply chains, accounting for more than 80% of international trade in goods. According to the United Nations Conference on Trade and Development (UNCTAD), in 2023, maritime trade volume increased by 2.4%, despite geopolitical uncertainties and the impact of the pandemic. The total port logistics market reached approximately \$371 billion, demonstrating steady growth, with a fore-

cast compound annual growth rate (CAGR) of about 3.9% by 2032 (Port Logistics Market Report | Global Forecast From 2025 To 2033).

In today's environment, digitalization and automation of port operations are becoming a top priority. The increasing volume of container traffic has led to a need for a shift from manual operations to autonomous systems that can ensure continuous operation and high levels of accuracy. One such solution is the use of AGV (automated guided vehicles),

which are electric self-propelled platforms that move containers horizontally between the dock and the back areas of the terminal. These vehicles can reduce operating costs and eliminate the impact of human error, while also reducing local emissions to zero.

The development of the smart port concept involves integrating automated guided vehicles (AGVs) into a single digital system that combines terminal management systems (TMS) and port community system (PCS). This integration, combined with the principles of just-in-time (JIT) scheduling and digital twin technologies, ensures the synchronization of ship arrivals, optimization of energy use, and increased port capacity. As a result, automation not only enhances efficiency but also contributes to environmental and energy sustainability.

This study aims to identify key trends and scenarios in the development of port logistics through digital transformation, explore the role of AGVs in shaping a smart, environmentally friendly port architecture, and assess the potential for their implementation in Russian ports in the Black Sea and Baltic regions.

### Theoretical foundations of port logistics

Port logistics is a complex system of organizational, technical, informational, and legal processes that facilitate the movement of

goods, ships, and vehicles through seaports as key nodes in global supply chains. Modern logistics theory views ports not only as transshipment points but also as integration platforms that bring together shipping lines, terminals, customs services, freight forwarders, and transport corridors in a unified digital ecosystem. The effectiveness of this system relies heavily on the level of digitalization, standardization of data exchange, and automation of processes. By leveraging technology, ports can optimize operations, reduce costs, and improve efficiency, ultimately contributing to the overall success of the supply chain.

The key element of the port's digital ecosystem is the Port Community System (PCS), an open and neutral electronic platform that brings together public and private stakeholders in the port (including administrations, terminals, shipping lines, forwarders, and customs) to facilitate intelligent and secure data exchange. The platform operates on the principle of "single entry – multiple use", allowing users to access and share information in a secure and efficient manner. The figure below illustrates the architecture of the port community and the Port Community System, which brings together all key participants in the logistics chain, including port authorities, terminal operators, shipping lines, freight forwarders, and customs.

**Figure 1.** The structure of interaction of participants in the Port Community System (Port Community System | Port Economics, Management and Policy)



In the smart port operating architecture, a bundle of PCS–TMS, AGV, and STS forms a cyber-physical system. PCS and TMS coordinate tasks, while AGVs provide autonomous horizontal movements of containers, and STS cranes perform vertical operations. At the current level of development, STS cranes are often the “bottleneck” because they require the participation of a human operator. The next step is to automate them in a single control loop, which will reduce the need for human intervention.

From the point of view of comparative assessment and benchmarking, two indices are used: the LSCI (Line Shipping Connectivity Index) from UNCTAD and the CPPI (Container Port Performance Index). The LSCI measures a country or port’s “embeddedness” in the liner-shipping network, taking into account factors such as frequency, vessel capacity, and number of services. The CPPI, on the other hand, measures the efficiency of ports based on ship time in port and processing performance. In 2023, countries with the highest connectivity according to the LSCI included China, the Republic of Korea, Singapore, Malaysia, and the United States. These countries demonstrate a concentration of capacity and network effects in their East and Southeast Asian hubs, as well as North American hubs, according to this index (Maritime transport indicators).

### **Current trends and technologies in port logistics**

Modern port logistics are undergoing a significant technological transformation, driven by the shift from disparate information technology (IT) solutions to integrated, digital smart port ecosystems. This transformation is being driven by the automation of overloading operations, predictive analytics, data integration, and the implementation of cyber-physical management models. Digitalization is becoming essential for the sustainability and competitiveness of ports, as it helps them adapt to global trade volatility and increasingly stringent environmental regulations.

The technological vector is shaped by three interconnected areas: first, the complete or partial automation of terminals, including electrified automatic gantry cranes and autonomous AGV vehicles, as well as remote control of transshipment equipment. Second, the introduction of tools for synchronizing ship loading and predictive analytics, such as ETA/ETD. Third, the creation of digital replicas of the port’s infrastructure and operations, which optimize mooring, towing, berth planning, and rear-area processing.

The most significant example of the integration of these technologies is Tuas Port in Singapore, the world’s largest fully automated terminal, which operates hundreds of electrified AGVs and automated cranes with centralized control from a single digital center. The system provides round-the-clock operation, reduces greenhouse gas emissions by almost 50% compared to its diesel counterparts, and creates new high-tech jobs. The project is being implemented under the management of PSA Singapore in cooperation with the A\*STAR research agency, where AGV flotilla coordination algorithms based on high-performance computing have been developed (Maritime & Port Authority of Singapore (MPA)).

In Europe, the port of Rotterdam, where the Port Xchange platform operates, serves as an example of the implementation of digital management tools. This platform provides real-time data exchange between shipping lines, terminals, and port services, allowing for the synchronization of ship arrivals and operations at berths based on the Just-in-Time Arrival principle. This approach helps reduce downtime, fuel consumption, and improves the accuracy of port resource planning. Combined with digital counterparts, the Port Authority of Rotterdam has created a “forecasting management” model where all participants operate in a unified information space.

Table 1 presents the key technological trends in port logistics along with verifiable examples.

**Table 1.** Key technological trends in port logistics and verifiable examples

The trend	Content / effect	Examples
Automation of port terminals	The introduction of automatic cranes, autonomous vehicles (AGVs), and digital warehouse management systems increases productivity and reduces the impact of human error.	In 2023, the largest automated terminal in the world with electrified automated guided vehicles (AGVs) and remotely operated cranes, PSA Singapore, is operating at the Tuas Port in Singapore.
Synchronization of ship arrivals (Just-in-Time Arrival)	Using digital platforms to coordinate ships, terminals, and services, we can reduce downtime and fuel consumption.	PortXchange (Rotterdam, Hamburg) is a platform for exchanging ETA/ETD data in real time, integrated with AIS and port systems
Digital port twins	Real-time modeling of port infrastructure and data flows, as well as forecasting berth loading, towing, and transshipment operations.	The Port of Rotterdam Digital Twin is a system that visualizes the water area, depth, traffic, and weather data. It is used to optimize shipping schedules and calls.
Internet of Things (IoT) and Predictive Analytics	Monitoring of equipment and cargo using sensors; analysis of data to prevent downtime and optimize routes.	The Hamburg Port Authority has introduced the SmartPort Logistics platform, which uses IoT (Internet of Things) devices and analytics to manage traffic and ships.
Artificial intelligence and machine learning	They are used for estimating the expected time of arrival (ETA), planning crane operations, analyzing container flow, and monitoring energy consumption.	DP World has implemented AI systems at its Jebel Ali and London Gateway terminals, and in Singapore, PSA Marine is using ML algorithms to optimize tugboat operations.
Blockchain and electronic documents	Ensuring transparency and security in supply chains, and reducing the time of customs procedures.	TradeLens (IBM + Maersk) and CargoSmart are used in Asia and Europe to facilitate document exchange between shipping lines and port authorities.
Environmental Technologies (Green Ports)	Electrification of equipment, use of renewable energy sources, and coastal power supply for ships (OPS).	The ports of Los Angeles and Gothenburg have installed OPS systems to reduce CO <sub>2</sub> emissions from ships when they are in port.
Port Community System (PCS) Integration	A centralized digital platform for all participants in the logistics chain, including customs, terminals, agents and carriers.	In 2023, PCS systems will be fully implemented at the Antwerp-Bruges, Rotterdam, and Valencia port complexes. These systems will provide the exchange of more than 20 million messages per day.

*Source: author's development*

AGVs have already demonstrated positive effects in container terminals in various countries, including increased processing speed, reduced operational costs and injuries, and improved environmental perfor-

mance. A comparison between a port without an AGV system and a port equipped with AGVs is presented below, highlighting key economic and operational indicators (Table 2).

**Table 2.** Comparative characteristics of ports without AGV and with AGV

Indicator	Port without AGV	Port with AGV
Organization of work	Manual control, human factor in planning and executing operations.	Fully automated ground logistics management via TMS/PCS in 24/7 mode, without shifts or downtime.
Capital expenditures (CAPEX)	Low initial investment in machinery and infrastructure.	High investments (tens of millions of dollars per terminal) are made in electric platforms and IT infrastructure.
Operating costs (OPEX)	High fuel, repair, and personnel costs.	Reduction of operating costs by 20–30% through the use of electric traction and minimization of staffing.
Efficiency	Shift work, high dependence on personnel and weather conditions	Increased container handling speed by 15–25%, 24/7 steady operation.
Safety	Risks of incidents and human error	Reduced injuries and errors thanks to autonomous movement and sensory control.
Environmental friendliness	Internal combustion engine use, high noise and emissions (No <sub>x</sub> , PM)	Electric drive – zero local emissions, reduced noise and vibration.
Flexibility and adaptability	The possibility of operational decisions by the operator, but low predictability of the system	High predictability and accuracy in tasks, with limited room for improvisation.
Image and compliance with environmental standards	Limited IMO and ESG compliance	«Green» image and compliance with environmental initiatives, as well as IMO-2030 requirements.
Return on investment	Slow efficiency improvement with rising costs	The average payback period for this investment is 3–5 years, thanks to the savings and increased efficiency it brings.

*Source: author's development*

The transition of global port logistics towards sustainable development is closely linked to the increasing international environmental regulations and the introduction of energy efficiency standards. Since January 1, 2023, the International Maritime Organization (IMO) has implemented mandatory

indicators, EEXI (Energy Efficiency Existing Ship Index) and CII (Carbon Intensity Indicator), to reduce the carbon footprint of ships. These measures encourage shipping companies and ports to optimize shipping speeds, plan ship calls digitally, and improve infrastructure efficiency. Ports that integrate



digital control systems and automated technologies gain a competitive advantage by accurately calculating energy use and predicting mooring windows with greater precision.

The European Union has introduced the FuelEU Maritime Regulation and the Fit for 55/AFIR block of measures, which require the mandatory use of onshore power supply for certain types of ships by 2030. These measures also include the development of standardized electrical infrastructure in ports of the TEN-T network. These initiatives aim to promote the transition to green technologies and require ports to install energy-monitoring systems and implement intelligent load management and power redundancy measures (EEXI and CII – ship carbon intensity and rating system).

The practice of terminal automation has been confirmed by industry research, which has identified semi-automated and fully automated systems. Semi-automated systems involve human control of horizontal logistics and automated warehousing, while fully automated systems perform both horizontal movements and vertical processing without human intervention.

These systems are being implemented on a large scale in Asia and several European hubs, and are linked to increasing demands for the integration of transportation management systems (TMS), shift planning systems, and cybersecurity measures. Systematic reviews have identified significant benefits in terms of security and operational stability, but also emphasize the need for process redesign and staff training to ensure successful implementation (Container Terminal Automation).

#### **Environmental and sustainable aspects of port logistics development**

The transition of port logistics towards sustainable development has become a priority for the global transport industry. The main directions of environmental transformation in port logistics are:

- Onshore Power Supply (OPS) – connecting ships to electricity in the port to reduce CO<sub>2</sub> and NO<sub>x</sub> emissions. By 2023, this system will be implemented at ports in Los Angeles, Gothenburg, Rotterdam, and Hamburg;

- Electric AGVs – as part of a “zero-emissions” fleet, they can reduce noise pollution and eliminate local NO<sub>x</sub>/PM emissions, which is important for ports located in urban areas;
- Alternative fuels – the use of LNG (liquefied natural gas), biofuels, hydrogen, and ammonia for port equipment and ships;
- IMO EEXI and CII – regulations for energy efficiency and the carbon index of ships that affect port schedules;
- Digital energy management – implementation of systems for monitoring and optimizing the use of electricity and terminal resources;
- Development of green shipping corridors – creation of international routes with minimal emissions (Clydebank Declaration initiative);
- Recycling and zero waste – recycling and reuse of packaging and construction materials in ports;
- Green certificates and ESG reporting – transition of port operators to sustainable development reporting standards (GRI, ESG index);
- Cooperation with city authorities – integration of ports into urban environmental infrastructure (wastewater treatment systems, noise reduction, greening of coastal areas).

These measures form the foundation for the transition of the global port system from a “growth-driven” model to a “sustainable and digital development” model. In this new model, efficiency is measured not only by the volume of cargo handled, but also by how well the infrastructure reduces its carbon footprint and promotes sustainability.

#### **Geo-economic and political factors of the future of port logistics**

Modern port logistics operate in a highly turbulent global economic environment, which directly impacts the strategies for technological renewal. The increased sanctions policy, fluctuations in currency values, rising energy costs, and disruptions to international supply chains all require ports to reconsider their development priorities. Intangible risks, such as cyber threats, also play a significant role, as they can destabilize operational



processes and lead to temporary infrastructure blockages. Against this backdrop, the policies of technological sovereignty, digital security, and localization of critical components are becoming increasingly important. Investments in automation and digitalization are not just tools for optimization, but mechanisms for protecting against external risks. The use of autonomous vehicles (AGVs) integrated into port management systems (TMS and PCS) minimizes dependence on human factors, increases the stability of logistics operations, and ensures the predictability of cargo flows, even under external shocks.

For the ports of the Black Sea region, it would be beneficial to consider introducing AGVs as a key part of the modernization of land transportation systems in order to reduce costs, increase resistance to peak loads, and ensure the continuity of the transportation process. The most important factors for the successful implementation of such projects include access to qualified technical support, the establishment of reliable supply chains, and the gradual localisation of production and maintenance of equipment.

### **Forecast scenarios and directions of port logistics development**

The basic scenario for the development of port logistics in the coming years involves a phased approach to automation. At the first stage, autonomous AGV (automated guided vehicle) vehicles will be introduced and land logistics will be digitalized. At the second stage, STS (ship-handling) cranes will be automated within a single TMS (terminal management system) control loop.

This sequence ensures a balance between technological risks and investment opportunities, as well as the rate of return on capital investments. In combination with JIT (just-in-time) synchronization mechanisms and digital twins, port systems can form predictable arrival windows, optimize operation planning, and create smoother energy consumption profiles at terminals. This, in turn, helps reduce operational peaks, improve resource utilization, and enhance the overall sustainability of infrastructure.

Further development of automation in ports involves integrating AGV (Automated Guided Vehicles), STS (Ship-to-Shore) sys-

tems, and intelligent control systems into a unified cyber-physical ecosystem. Algorithmic control of data and energy flow is a key factor in ensuring efficiency. The transition to this model will allow ports to adapt to increasing cargo volumes, environmental reporting requirements, and the need for global competitiveness.

Automation technology is still in its early stages in Russian ports, but there is significant potential for development. The Black Sea and Baltic regions are promising areas for pilot projects, as they have high cargo turnover and large terminals. These areas can serve as a testing ground for AGV and digital TMS/PCS (Terminal Management System/Process Control System) systems.

The use of autonomous electric platforms can increase the stability of ground logistics, reduce operating costs, and ensure compliance with environmental standards, without the need for major infrastructure reconstruction. The localization of equipment production, the training of engineering personnel, and the development of service support all play an important role in implementing such projects.

### **Challenges and barriers to innovation**

The main obstacles to digitalization remain high costs, the fragmentation of information systems, and a lack of skilled IT personnel. Lack of trust between logistics chain participants and lack of uniform data exchange standards hinder integration. Additionally, for many ports, innovation can be economically risky due to long payback periods. These challenges can be addressed through public-private partnerships, standardization, and vocational education development.

### **Conclusion**

Port logistics is undergoing a period of significant structural transformation due to the combined impact of technological, environmental, and geo-economic factors. As global practice confirms, digitalization and automation have become essential components for the competitiveness of modern ports.

One of the key directions of development is the gradual automation of operations. This

includes the introduction of autonomous electric automated guided vehicles (AGVs) to optimize ground transportation, followed by the robotization of ship-to-shore (STS) cranes, creating a fully automated “side-to-warehouse” process. When combined with Just-in-Time (JIT) and Digital Twin technologies, this forms the basis for a cyber-physical system of a smart port where all processes can be managed in a unified digital space.

IMO and EU regulatory initiatives aimed at improving energy efficiency and reducing emissions are driving the electrification and digitalization of port infrastructure. These

initiatives include the use of AGVs (autonomous ground vehicles) and intelligent energy management systems, which make it possible to combine economic efficiency with environmental sustainability.

Russia has identified the development of automated terminals as a strategic priority. Pilot projects based on AGVs and TMS/PCS (transportation and traffic management systems) digital platforms in the Black Sea and Baltic Sea ports can serve as a basis for establishing national standards for smart and green ports that can integrate into international digital logistics networks.

## References

- Container Terminal Automation. [Electronic resource]. – Access mode: <https://metrans.org/assets/research/container%20terminals%20automation-final%20report-for%20metrans%20posting.pdf>.
- EEXI and CII – ship carbon intensity and rating system. [Electronic resource]. – Access mode: <https://www.imo.org/en/mediacentre/hottopics/pages/eexi-cii-faq.aspx>.
- Maritime & Port Authority of Singapore (MPA). [Electronic resource]. – Access mode: <https://www.mpa.gov.sg/home>.
- Maritime transport indicators. [Electronic resource]. – Access mode: [https://unctad.org/system/files/official-document/rmt2023ch4\\_en.pdf](https://unctad.org/system/files/official-document/rmt2023ch4_en.pdf).
- Port Logistics Market Report | Global Forecast From 2025 To 2033. [Electronic resource]. – Access mode: <https://dataintelo.com/report/global-port-logistics-mark>.
- Port Community System | Port Economics, Management and Policy. [Electronic resource]. – Access mode: <https://porteconomicsmanagement.org/pemp/contents/part3/digital-transformation/port-community-system/>.
- Review of Maritime Transport 2023. | UN Trade and Development (UNCTAD) [Electronic resource]. – Access mode: <https://unctad.org/publication/review-maritime-transport-2023>.

submitted 04.09.2024;

accepted for publication 18.09.2024;

published 8.10.2024

© Pavlikhin, A.

Contact: [impstudio@gmail.com](mailto:impstudio@gmail.com)

# Contents

## **Section 1. Electrical engineering**

*Rustamov Nasim Tulegenovich, Kibishov Adylkhan Talgatovich,  
Mukhamejanov Nuridin Baktiyaruly*

THERMAL AND ENERGY CHARACTERISTICS OF A COGENERATIVE FRACTAL SOLAR COLLECTOR.....	3
--	---

## **Section 2. Medical science**

*Polatova D. Sh., Artikhodzhaeva G. Sh.*

ASSOCIATED SOMATIC DISEASES IN PATIENTS WITH CERVICAL CANCER (SAMPLE ARTICLE) .....	11
--	----

## **Section 3. Technical ingeneral**

*Khaladdin Javadov*

EARTHQUAKE PREDICTION USING SHORT RADIOWAVE TECHNOLOGY.....	16
--	----

## **Section 4. Transport**

*Pavlikhin Andrey*

THE FUTURE OF PORT LOGISTICS .....	30
------------------------------------	----